Journal of Energy

ISSN 1849–0751 (On–line)
ISSN 0013–7448 (Print)
UDK 621.31

https://doi.org/10.37798/EN2021703

VOLUME 70 Number 3 | 2021

ENERGIJA 70

Journal of Energy

Scientific Professional Journal Of Energy, Electricity, Power Systems
Online ISSN 1849–0751, Print ISSN 0013–7448, VOL 70
https://doi.org/10.37798/EN2021701

Published by

HEP d.d., Ulica grada Vukovara 37, HR–10000 Zagreb

HRO CIGRÉ, Berislavićeva 6, HR–10000 Zagreb

EDITORIAL

This is the third regular issue in 2021, the year we celebrate the 70th anniversary of the Journal of Energy. We are particularly pleased that our journal has been included in the INSPEC (Information Services for the Physics and Engineering Communities) citation database for professional journals. INSPEC is a bibliographic database published by the Institution of Engineering and Technology (IET) in London that indexes and contains works in the fields of physics, electrical engineering, computer science, information technology, and engineering. This is a great motivation for the future work of the editorial board to achieve a better quality of works on various topics of energy and power systems.

The first paper, titled »Infrared Thermography in Steam Trap Inspection,« addresses the use of infrared thermography in preventive maintenance and periodic inspection of steam traps to increase reliability and reduce equipment downtime. The role of the steam trap is to separate the condensate and keep steam in the system, contributing to overall efficiency. Proper operation of the steam trap has a significant impact on reducing energy losses, which is why steam trap inspection plays an important role in plant maintenance.

The next paper, »Land Use and Energy Nexus,« discusses the land use-energy nexus from two perspectives: the impact of energy on land use and the impact of land use on energy. The impacts of energy on land use focus on direct and indirect land use changes resulting from vegetation clearing, topsoil destruction, and human relocation during the various phases of fossil fuel and uranium ore extraction, deposition, and transportation, as well as during the construction of renewable energy sources and associated structures (highways, dams, culverts, tunnels, power plant infrastructure, and energy transmission networks). On the impact of land use on energy, appropriate urban and transportation infrastructure and multi-energy systems are proposed as a solution to increase energy efficiency and ensure sustainable development.

The third paper is »Development of a LabVIEW - Based Data Logging and Monitoring Application for a Photovoltaic Power Plant at FER«. The paper describes the implementation of the LabVIEW programming language for the development of a graphical user interface (GUI) and visualisation of the collected measurements from photovoltaic inverters in a SCADA system in a university building. The developed software solution allows simple multiprocess operations performed at different speeds.

The fourth paper »Deep Neural Network Configuration Sensitivity Analysis in Wind Power Forecasting«. shows one of the approaches to apply deep learning to wind power forecasting using recurrent networks for sequential data. The process of data preparation and the data structure as well as the model structure are explained. Finally, a comparison of the forecasts obtained with the proposed methodology and commercial tools is presented with two examples, providing insight into the accuracy of the forecasts obtained with Deep Learning methods.

The final paper is »Cavitation Detection on Hydraulic Machines.« The paper gives a technical overview of the phenomenon of cavitation in hydraulic machines: turbines, pumps and ship propellers. Many researchers used different techniques such as visual methods, pressure and cavitation noise measurements, CFD methods to predict and analyse cavitation. Techniques for predicting cavitation erosion potential are also used. In general, each of the methods for detecting cavitation on hydraulic machines has advantages and disadvantages, and there are gaps that can be improved.

Goran Slipac
Editor-in-Chief

Journal of Energy

VOLUME 70 Number 3 | 2021

journal homepage: http://journalofenergy.com/

Hrvoje Glavaš [1]
Faculty of Electrical Engineering, Computer Science and Information Technology Osijek, Croatia
hrvoje.glavas@ferit.hr

Držislav Vidaković
Faculty of Civil Engineering Osijek
dvidak@gfos.hr

Igor Sušenka
igor.susenka@ferit.hr

Infrared Thermography in Steam Trap Inspection

1 Statements expressed in the paper are author's own opinions, they are not binding for the company/institution in which author is employed nor they necessarily coincide with the official company/institution's positions.

SUMMARY

Steam traps play a significant role in condensate evacuation from steam as well as in heating ventilation and cooling systems (HVAC), i.e., industrial climate chambers. Preventive maintenance and periodical audit of steam traps increase reliability and reduce the number of facility off hours. In some elements of the system, condensate can damage some parts, which means that monitoring their function is one of the basic preventive maintenance tasks. One way of checking steam traps is by using infrared thermography. The paper presents the simplicity of steam trap control by using an infrared thermography camera.

KEY WORDS

Key words: Infrared thermography, Steam trap, Maintenance

INTRODUCTION

As a contactless method for determining temperature distribution on the surface of the object under consideration by measuring radiation intensity in the infrared (IR) band of the electromagnetic spectrum, infrared thermography represents one of the ways of controlling the steam trap state. According to international standards, infrared thermography is classified as a non-destructive testing method (NDT), [1]. Every object heated to the temperature above absolute zero transmits EM radiation of a continuous spectrum of all wavelengths, and when the temperature exceeds 525°C, it emits visible light [2]. The application of an infrared thermographic camera is easier when the operator is educated in the field of thermography, but even then, there are possibilities of making a mistake. Mere knowledge of thermography is not sufficient but physical knowledge is necessary to understand the system in which thermographic analysis is performed. Steam traps are very important from a technical point of view, but from the energy aspect, they are imperative. Regular control of steam traps contributes to the overall maintenance of thermodynamic steam generating systems. It is estimated that 20% of generated steam is lost through defective steam traps, [3].

COMMON TECHNICAL SOLUTIONS

The basic function of steam traps is fast condensate evacuation, preventing the loss of working media (dry steam) and releasing accumulated air in the system, which is a thermal insulator. Steam traps are self-opening valves, which open in the presence of condensate and close in the presence of steam. They contribute to efficient transfer of heat energy, reduce corrosion in pipes and the occurrence of water hammer. Their task is to separate the condensate with reduced condensate cooling. Dimensioning is based on usage, differential pressure, working/starting capacity and steam temperature, [4]. The common application of steam traps in the thermotechnical system is represented in Figure 1, which also best illustrates a closed flow of condensate within the system [5].

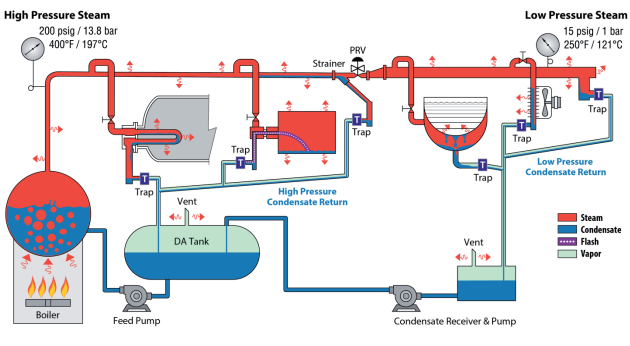

Figure 1. Steam trap in a thermotechnical system [5].

Steam traps requre periodic maintenance to ensure safety, quality of a production cycle and increased process efficiency. The experience of maintainers tells us that 20-25% of installed separators do not work properly.

Steam traps work well if the system is balanced, if there is enough steam at inlet and if the steam arrives at the steam trap. By their mode of operation, they are divided into continuous discharge steam traps and intermittent steam traps that work on the principle of collecting condensate leakage of content and closure of the valve.

The most common technical solutions are:

Hrvoje Glavaš, Držislav Vidaković, Igor Sušenka, Infrared Thermography in Steam Trap Inspection, Journal of Energy, vol. 70 Number 3 (2021), 3–7
https://doi.org/10.37798/2021703122

Bimetallic steam traps, Figure 2. Their advantage are small dimensions, but they have high condensate discharge capacity. One of their characteristics is also large starting capacity due to an open valve when it is cold. In addition, they suit well water hammer, corrosion, high pressure, and superheated water steam. They work within a high operating pressure range and can be maintained while connected to the system. The shortcomings are a slow operation mode and the possibility of excessive condensate cooling of at increased output pressure.

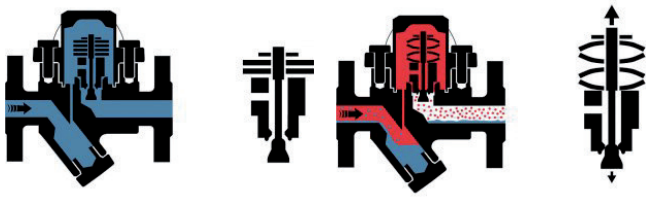

Figure 2. Bimetallic steam trap, cross section and principle of operation, [6]

Float type steam traps shown in Figure 3 are extremely reliable, but can lead to air accumulation. The advantages of a technical solution with thermostatic and floating type steam traps are as follows: continuous discharge of the condensate, which is at a steam temperature, at high and low loads it has good endurance, it is not affected by pressure changes, and it releases air. The shortcomings are as follows: constructive elements are susceptible to water hammer and they are not suitable for corrosive condensate and superheated water steam. Also, freezing can occur and the pressure determines the aperture.

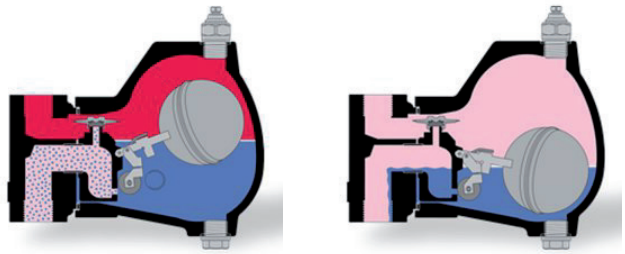

Figure 3. Condensate steam trap with float, cross section and the principle of operation, [6]

Inverted bucket steam traps, given in Figure 4, are one of the oldest solutions, their problem is the initial startup and steam release. The required force of operation ensures that steam enters the condensate bin until steam rises up and closes the valve. Steam passes through the hole in the canister, then condensates and ensures that the valve reopens and the condensate is discharged. This type of steam traps is used in high pressure systems and superheated water vapor, it is impact resistant, simply designed and easy to maintain. The disadvantage is that it has a slow discharge of steam that can lead to steam loss and sealing requires water in the body that is subject to freezing.

Figure 4. Inverted bucket steam trap cross section, [7]

Thermodynamic steam traps are small, Figure 5, (steam traps with disks). They work on a mechanical principle, using the pressure increasing and decreasing zones that raise and lower the disc. Thanks to the flow rate and the differential pressure, the steam and condensate flow stops. They are often used because they are cheap but may pose a problem in poorly regulated systems. The benefits are low cost and a wide range of high capacity utilization, plus they are compact and lightweight. They can be used in high-pressure superheated water vapor and are corrosion resistant. They are not affected by freezing and are easy to maintain because they have only one disk. The disadvantages are that a low pressure at the entrance or a high pressure at the outlet affects the operation. Cooling of the operating chamber due to a low outdoor temperature or rain results in faster condensation of an accelerated operation and premature wear. They are also noisy and lead to energy loss.

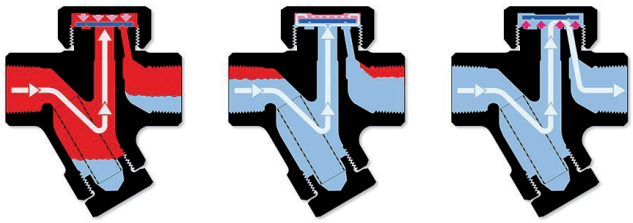

Figure 5. Thermodynamic steam traps, cross section and the operation principle, [6]

Thermostatic steam traps, Figure 6, allow easy separation of air, quickly and without loss. This type of steam trap uses a bimetallic delta loop that combines thermodynamic and thermostatic forces for larger amounts of condensate. They use pressure and temperature for operation and have a modulated output.

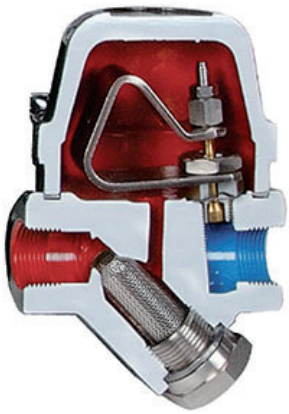

Figure 6. Thermostatic bimetallic delta element steam trap cross section [7]

STEAM TRAP STANDARDS

To the best of our knowledge, there are six European and six ISO standards defining the basic requirements placed on steam traps and these are: ISO 6552: 1980 Automatic Steam Traps - Definition of Technical Terms; This international standard gives definitions of the main technical terms and expressions used to describe automatic steam traps regarding dimensions, pressure, temperature and flow as well as their respective symbols and units. EN 26553: 1991 - Its purpose is to establish certain basic requirements for marking steamers and give recommendations for additional information marks. In general, consideration should be given to specific requirements that can be agreed upon by the respective partners. It sets mandatory and optional tags for steam traps. (ISO 6553: 1980 Automatic steam traps - Labeling - withdrawn). EN 26554: 1991, ISO 6554: 1980 -Automatic air steam traps with flanges - face-to-face dimensions. EN 26704: 1991, ISO 6704: 1982 - Classification of steam traps. EN 27841: 1991, ISO 7841: 1988 - Methods for determining vapor losses of automatic steam traps. ISO 7842: 1988 - Determination of the capacitance of discharge automatic steam traps. EN 26948: 1991 ISO 6948: 1981 - Performance tests for automatic steam traps.

Hrvoje Glavaš, Držislav Vidaković, Igor Sušenka, Infrared Thermography in Steam Trap Inspection, Journal of Energy, vol. 70 Number 3 (2021), 3–7
https://doi.org/10.37798/2021703122

MAINTENANCE SAVINGS

Studies published in [3] indicate that 20% of the generated steam is lost through improper steam traps. Regular preventive maintenance of the system is necessary because the proportion of defective steam traps increases over the years. This is presented best in Figure 7. Potential savings of preventive maintenance can be derived from the statistics referring to the corrected malfunctions.

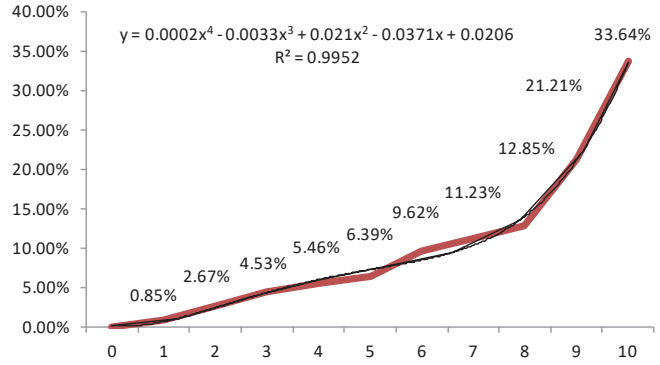

Figure 7. Percentage of steam trap breakdown over a period of 10 years, [8]

STEAM TRAP TEST METHODS

Steam traps are commonly tested in three ways: visually, by ultrasound and by infrared thermography. By applying all three testing methods we come to the best results [9]. Ultrasound testing is most commonly used because it is a fast simple and accurate method, which is the only disadvantage that requires education and experience [9]. The ultrasound frequency used for steam traps ranges from 20 to 25 kHz [10]. Steam traps is essentially a valve that automatically discharge condensate when it comes to its accumulation. In Figure 8, we can see the signal level in the ultrasonic valve test.

Figure 8. Ultrasonic valve testing and measured values

Apart from the level of signal, the shape of the signal is essential for interpretation. Figure 9 shows the shape of the signal taken from [11], where opening, discharge of condensate and closure are colored magenta, yellow and cyan, respectively. In the case of a defective open damper, the signal is continuous with the shape shown in yellow, and in the case of a defective enclosure, we have a slight noise. It may be concluded from the signal format [11] if the steam trap does not have sufficient capacity, if it is overloaded due to malfunctioning of other system elements or if it is corrupted.

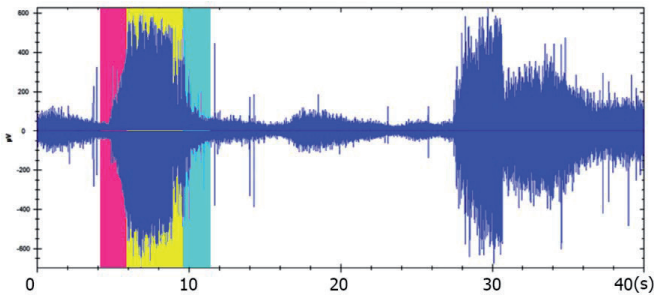

Figure 9. The steam trap signal shape in the correct operating mode

Ultrasonic analysis in practice is preceded by infrared thermography. A thermographic audit includes the analysis of the apparent temperature of the input and output openings, i.e., the determination of the temperature difference. IC thermography assists best in the analysis of thermodynamic steam traps, while in more complex structures it does not provide more information. It neither provides sufficient information for traps where the condensate passes continuously and in the case of a steam trap close to the condensate line. Delta T temperature measurement is a rough indicator of trap condition because small and moderate leaks cannot be detected [12]. Thermal analysis begins on the inlet pipe in the steam trap.

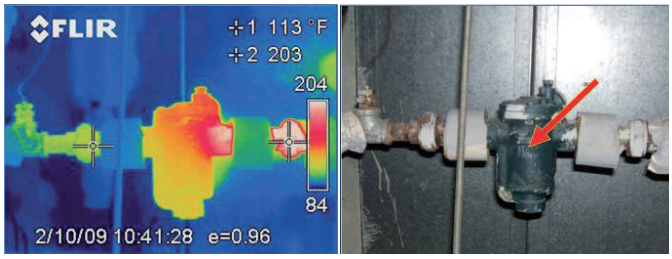

Figure 10. Thermogram of the clogged inverted bucket steam trap [13]

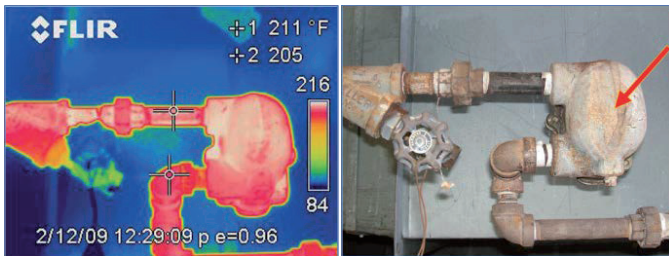

Figure 11. Thermogram of a leaking float ball steam trap with [13]

The inlet pipe temperature should be close to the steam temperature to the system, indicating that the steam comes in the steam trap and is not locked or defective in the closed position. If the temperature of the inlet pipe is considerably lower than the steam temperature, the steam does not reach the trap and it is necessary to investigate the cause. It occurs most often because of the closed valve before the steam trap, but the barriers within the pipeline can also prevent vapor flow. The condensation temperature should be monitored during the test. Figure 12 shows a typical temperature limit values for a given amount of condensation overpressure [14].

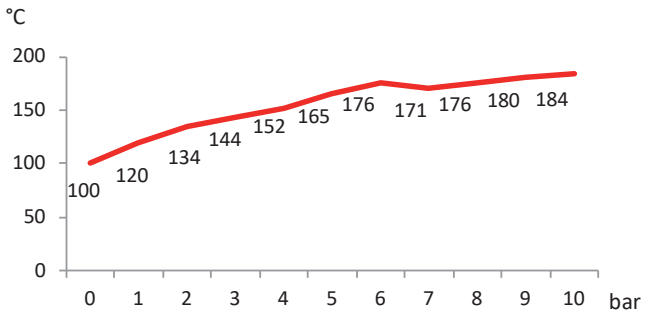

Figure 12. Temperature limit values

It can be concluded from a before mentioned that the pressure information within the analyzed part of the system is necessary for a successful thermographic analysis. The infrared thermal camera is especially useful for finding quickly closed valves or steam lines jamming, [12].

TESTING THE STEAM TRAP WITH GESTRA TRAPtest VKP 40

The GESTRA TRAPtest VKP 40 measuring device detects and analyzes the ultrasound produced by the steam trap and the connecting pipes. Measurements are made by selecting the type of the steam trap and by pushing the tip of the probe onto the trap. According to empirically established limit values, ultrasonic vibration are analyzed. Provided that the specified system pressures are known steam trap state can be analyzed and temperature information can be obtained, [15]. Figure 13 shows the test procedure.

Hrvoje Glavaš, Držislav Vidaković, Igor Sušenka, Infrared Thermography in Steam Trap Inspection, Journal of Energy, vol. 70 Number 3 (2021), 3–7
https://doi.org/10.37798/2021703122

Figure 13. Conduction of measurement

Measurement results are transferred to the computer and displayed as a report. Figures 14, 15 and 16 can be seen as typical records for particular situations inside the system. In the diagrams, we can see distinctive lines. The green line in the diagram represents the beginning of the active threshold line value TV measurement zone. If the measurement is this value it is possible to not have flow/load thru trap. Ideally, the measurement curve is below the TV, which is in practice, not a rare case. The red line represents the upper limit of the line value LV of measurement accuracy (not necessarily device malfunction).

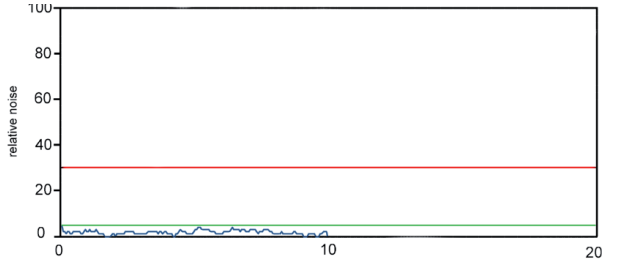

Date	Test results	Tester	Mean value	Limit value	Threshold
15.3.2019.	Cold (Result)		1	30	5

Figure 14. Steam trap is off or without flow/load

Figure 14 represents the stationary condition of the steam trap in which the steam supply is physically disabled (most often by the manual valve or an automatic valve operator). The device displays a blue vibration curve transmitted to the trap through the connecting pipes (or various brackets/fixers) connected to the trap. Figure 15 shows the case when most curves are above the upper limit and the trap does not perform its function properly. A similar curve can be observed in the cases of noise transmission from the ″foreign noise″ system, in which the external factor affects the measurement. The problem can be resolved by experience or by using software that comes with the device.

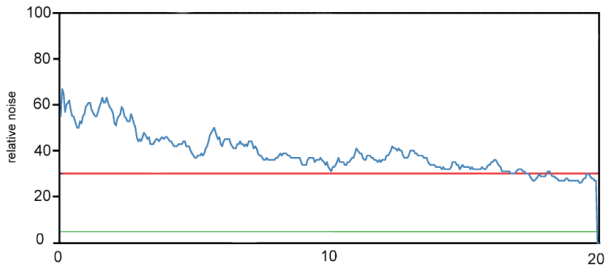

Date	Test results	Tester	Mean value	Limit value	Threshold
15.3.2019.	Defective		39	30	5

Figure 15. Steam trap does not perform its function properly

Figure 16 illustrates the case of the normal functioning of the steam trap. Most curves are below the upper limit, which suggests that the trap performs its function properly, but there are indications of wear. The shape of the curve indicates possible noise pollution or potential wear due to the manufacturing date of the device.

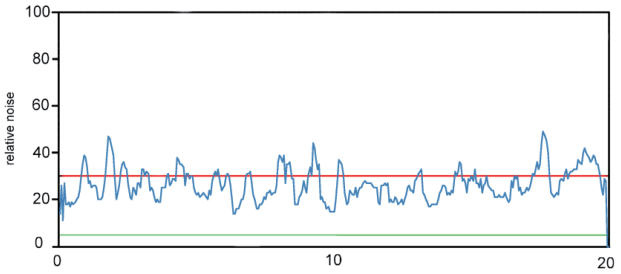

Date	Test results	Tester	Mean value	Limit value	Threshold
15.3.2019.	OK		26	30	5

Figure 16. Steam trap performs the function properly

THERMOGRAPHIC ANALYSIS OF STEAM TRAP

For the paper, a practical test of the float ball steam trap was initially carried out with infrared camera Fluke Ti200. The basic characteristics of the camera are: resolution 200x150 pix, FOV 24 ° H x 17 ° V, IFOV 2.09 mRad, thermal sensitivity 75 m ° C, measuring ranges from -20 ° C to +650 ° C. The test results can be seen on the thermograms shown in Figure 17, Figure 18 and Figure 19.

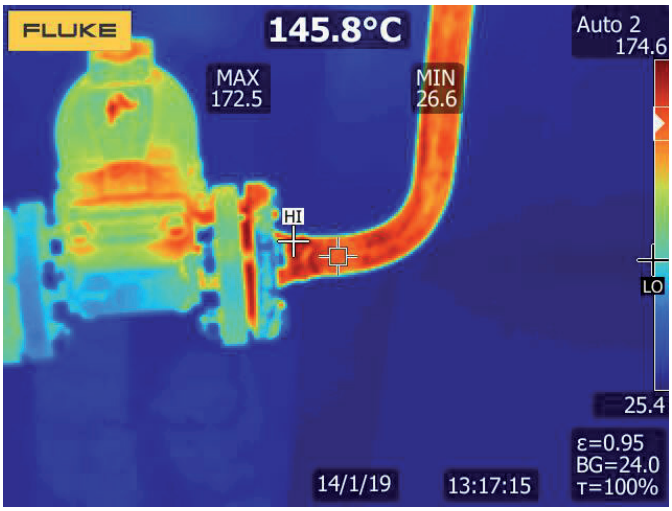

Figure 17. Apparent temperature at the inlet

Figure 17 shows the maximum amount of measured apparent temperature at the inlet of a separator of 146 °C. Figure 18 indicates that the outlet water temperature of 94 °C. At the time of recording the pressure in the system was 3 bars.

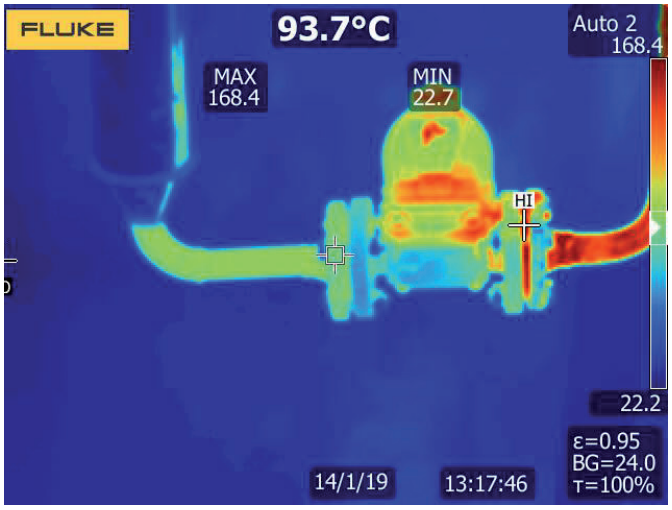

Figure 18. Apparent temperature at the outlet

Hrvoje Glavaš, Držislav Vidaković, Igor Sušenka, Infrared Thermography in Steam Trap Inspection, Journal of Energy, vol. 70 Number 3 (2021), 3–7
https://doi.org/10.37798/2021703122

Based on the data from Figure 12, we can conclude that water vapor arrives at the inlet of the steam trap, and the temperature difference of 52 °C suggests the correct operation. The float ball steam trap represents a technical solution of the continuous flow. In the case of malfunction/jamming, the output temperature would be significantly smaller, and in the case of openness, it is significantly higher. In Figure 11 showing the aperture we have a temperature difference of 3 °C; at the inlet, it is 99 °C (211 ° F) and at the outlet, it is 96 °C (205 °F).

The temperature values displayed by an infrared thermocamera are called apparent temperatures because the camera measures the amount of infrared radiation that the temperature parameter assigns to the temperature value. The parameters that most influence the wrong reading in our case are the wrong choice of material emissivity and angle of recording. In Figure 17, the maximum recorded temperature is 173 °C, while in Figure 18, the maximum apparent temperature is 168 °C. This is a temperature difference of 27 °C between the measured point and the maximum value recorded by the camera. That is why it is very important to do multi-angle analysis to eliminate measurement errors because they can lead to wrong conclusions. This temperature difference corresponds to the equivalent difference of more than 2 bars within the pipeline and incorrect interpretation of the apparent temperature may misrepresent the steam condition in the inlet water.

Figure 19 represents additional control measurement, confirming of conducted testing. For a proper interpretation, it is necessary to analyze the thermal recordings in software, taking into account the camera's resolution and IFOV (Instantaneous Field of View), which determines the spatial angle of each IC sensor element. The area where the apparent temperature is measured must be greater than IFOV.

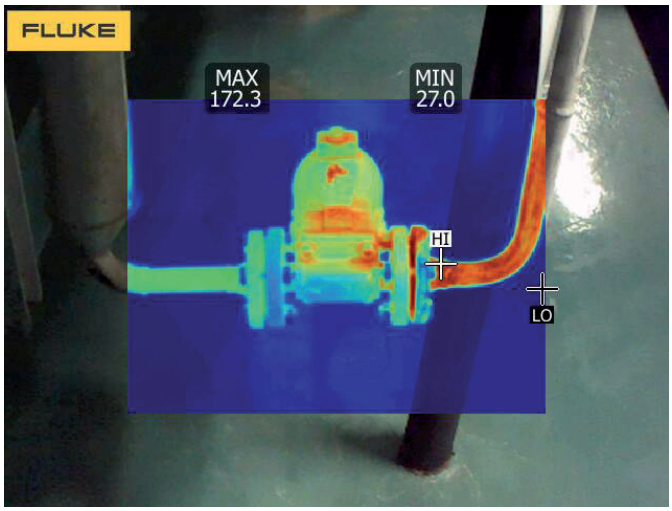

Figure 18. Steam trap analysis check

The biggest problem in thermographic testing are the metal parts upon which it is difficult to determine emissivity and apparent temperature values. This problem can be solved by placing reference points (tags) or painting measuring spots with the color of the known emissivity. From the displayed thermograms it is not possible to estimate the status of the operating trap, decay/wear of the trap that performs its function properly, that can be easily seen in Figure 16, by using the TRAPtest VKP 40.

CONCLUSION

Steam traps play a significant role in maintaining the reliability of the system's operation in which the condensate vapor separation is necessary. Steam is an invisible medium that transmits energy. When we can see steam, we talk about wet steam, i.e., condensate. The task of the steam trap is to separate the condensate and preserve the steam in the system and thereby contribute to overall efficiency, i.e. energy savings. Energy losses due to defective traps reach up to 20% of the energy invested in steam generation. Energy savings are the primary reason for preventive maintenance and trap testing, and the secondary increase of system reliability because it reduces the number of failures and prolongs life expectancy.

The steam trap test can be carried out by visual inspection, ultrasonic inspection and by a thermographic camera. The visual method is not reliable because by steaming it condenses, so it is difficult to estimate the amount of liquid phase in the condensate. The ultrasonic analysis is the most accurate form of testing that produces reliable results if the examiner has enough knowledge and experience. Despite the simplicity and the knowledge of system operation, Infrared thermographic analysis is not able to provide us information about the inside status of the steam trap. An exception is thermodynamic steam traps because they have a working member close to the casing surface. Another problem with the use of infrared thermography is the choice of emissivity, which is difficult to determine due to the presence of metal surfaces. This problem can be resolved by using reference tags and applying paint to metal parts, but this undermines the idea of the advantage of fast and contactless methods because reference markers and colorants have to be refreshed regularly due to a high working temperature of the system.

Regardless of whether infrared thermography is absolutely reliable in determining the condition of the steam trap, it is the first step of the trap testing because defective traps can be easily identified in order to reduce energy losses and it is the main reason why infrared thermography is irreplaceable test method.

REFERENCE

[1] H. Glavaš, T. Barić, M. Stojkov, ''Application of infrared thermograpy in technical systems, Proceedings'', 15th Natural Gas, Heat and Water Conference, 8th International Natural Gas, Heat and Water Conference, ISSN 1849-0638, HEP Plin, University of Osijek, University of Pecs, 33-50, 2017

[2] H. Glavaš, M. Vukobratović, M. Primorac, D. Muštran, ''Infrared Thermography in Inspection of Photovoltaic Panels'', International Conference on Smart Systems and Technologies 2017 (SST 2017), Faculty of Electrical Engineering, Computer Science and Information Technology Osijek, 63-68, 2017

[3] A. Messer, UE Systems DMS Steam Report, 2017, http://www.uesystems.com/steam-trap-inspections-reporting, UE Systems INC, 2017., accessed: 2. March 2019.

[4] Lesman Instrument Company, Steam Traps 101: Basic Technology and Applications, accessed: 11. April 2013.

[5] Amstrong International Inc, 2015, Steam Trap Selection, 856-EN, USA

[6] https://www.gestra.com/products/valves/a1-steam-traps.html, accessed: 2. March 2019.

[7] https://www.bestobell.com/front/products/?id=67, accessed 2. March 2019.

[8] Embedded Energy Technology, 2014, Steam Trap Inspection vs. Monitoring Comparing Preventative and Predictive Maintenance Approaches'', Pittsburgh, PA

[9] K. Paffel, Swagelok, (2014), Steam Trap Testing with Ultrasound, UE Systems INC

[10] UE Systems Inc, Steam Trap Testing, Pt. 1, http://www.uesystems.eu/articles/steam-trap-testing-pt-1, accessed 2. March 2019.

[11] SDT Ultrasound Solutions, 2014, Introduction to Steam Trap Testing'', https://youtu.be/ UisN8bazJ9w, accessed: 2. March 2019.

[12] R.J. Seffrin, Non-Destructive Testing of Steam Traps, https://www.irinfo.org/10-01-2017-seffrin, accessed: 2. March 2019.

[13] ThermoTesT, Ultrasonic/Infrared Steam Trap Testing, http://thermotest.com/services/infrared-applications/steam-analysis-and-steam-trap-testing, accessed: 2. March 2019.

[14] https://www.valvesonline.com.au/references/steam-tables, accessed 2. March 2019.

[15] GESTRA AG, (2005) GESTRA Steam Systems VKP 40Ex VKP 40 Operating instructions 818535-01

Journal of Energy

VOLUME 70 Number 3 | 2021

journal homepage: http://journalofenergy.com/

Md. Abubakkor Siddik[1]
Department of Land Record and Transformation
Patuakhali Science and Technology University
masiddik@pstu.ac.bd

A.K.M. Mostafa Zaman
Department of Agronomy
Patuakhali Science and Technology University
mostafazamanpstu@gmail.com

Land Use and Energy Nexus

1 Statements expressed in the paper are author's own opinions, they are not binding for the company/institution in which author is employed nor they necessarily coincide with the official company/institution's positions.

SUMMARY

In this research, the connection between land use and energy has been discussed from two points of view, i.e., the impacts of energy on land use and the impacts of land use on energy. This research identified several direct and indirect land use changes that occur by clearing vegetation, destroying top soils, and relocating human populations during the different stages of extraction, deposition, and transportation of fossil fuels and uranium ore; and during the establishment of renewable energy sources including wind turbines, hydro-power plants, and associated structures (highways, dams, culverts, tunnels, power station infrastructure, and energy transmission networks). Likewise, feedstock cultivation, processing, and transportation to biomass plants, as well as the production of biodiesel from municipal solid waste, require accessible land resources that further contribute to global land-use change. In the case of the impacts of land use on energy, mixed use development was found to be one of the most efficient approaches to achieve energy efficiency. Similarly, energy demand for motorized travel can also be reduced with the development of urban blocks and transit-oriented development. Furthermore, integrated combined heat and power systems, green space, and energy-supporting land use regulations were identified as energy savings strategies that may aid in achieving energy efficiency and ensuring sustainable development.

KEY WORDS

Land use, energy efficiency, fossil fuels, renewable energy, mixed use, green spaces

1. INTRODUCTION

Land is considered as a physical entity by means of topographical and spatial characteristics. It is the utmost gift of nature and is categorized as the fundamental resource of human society [1]. Land formed between 480 and 360 million years ago during the mid-Palaeozoic era [2]. It supports population growth, economic and societal development. Land use is usually defined as the human utilization of land. It is also considered as the modification, alteration, and management of natural environments into built environments such as settlements, agriculture, transportation, industry, recreation, and open space [1], [3], [4]. Land use change or land transformation is a major concern for the betterment of the healthy wellbeing of human society. It is the outcome of environmental conditions and socio-economic, cultural, political, and institutional conditions as well as the interaction of the determinants [5], [6]. However, anthropogenic alteration that is for socio-economic wellbeing has been reported as the most influential for land use change through the processes of demographic change, industrialization, urbanization, economic and technological improvement, institutional factors, cultural factors, and globalization [5], [7]–[11].

Energy has been considered as the central determinant for smooth economic development and people's livelihood in Bangladesh and many other countries [12], [13]. However, the world's energy systems are evolving with new smart energy and grid technologies [14]. This energy can be derived from oil, gas, hydropower, solar, nuclear, geothermal, and other types of energy with the aim of generating electricity for lighting homes, offices, industries, etc. and operating/charging appliances; powering automobiles; and running the industry [15]. Extraction of fuel (oil/coal/gas), storage, construction of production infrastructure, the production and distribution processes, including uses of neighboring land and waste disposal, have different land use impacts and environmental implications [16]. By 2050, the global urban population is expected to grow by almost 2.5 billion people. Asia and Africa will house nearly 90% of the newly added population. These additional populations need more new and improved housing and associated infrastructure, leading to a significant increase in energy consumption [17], [18]. To meet these challenges, people need to go for energy efficiency or efficient energy use, which basically defines using less energy to carry out similar work, and this way energy waste can be eliminated. The main aim of energy efficiency is to diminish the amount of energy required for producing goods and services [19]. The tools and techniques of land use have impressive potential to reduce a community's energy consumption and are also required for improving the economy and mitigating climate change [20]. Hence, this chapter focuses on the nexus between land use and energy.

2. METHODS

Researchers searched related literature using different academic databases and search engines, including Scopus, ScienceDirect, Web of Science, PubMed, Google Scholar, and ScienceOpen. For considering the aspects relevant to the nexus between land use and energy, various search combinations were performed using different keywords such

Abubakkor Siddik, Mostafa Zaman, Land Use and Energy Nexus, Journal of Energy, vol. 70 Number 3 (2021), p. 8–13
https://doi.org/10.37798/202170361

as land use, energy, fossil fuels, renewable energy, nuclear power, mixed use, transit-oriented development, green spaces, hydro-power, biomass, biodiesel, combined heat and power systems, urban block development, and energy-supporting land use plans and policies. Searching was done in the early 2022 and considered literature written in English. The outputs were manually screened, and duplicates were removed. After that, researchers finalized the relevant literature to perform the review after rereading abstracts, and in some cases, methodology and conclusion parts. The results of this review are presented in Section 3 (land use and energy nexus). In the sub-sections (3.1 and 3.2), a detailed description of the consequences of energy sources and their associated infrastructure on land use as well as implications of land use on energy, particularly energy efficiency, is provided. Finally, in Section 4, some concluding remarks are presented.

3. FINDINGS: LAND USE AND ENERGY NEXUS

There are two different views on the nexus between land use and energy, i.e., (a) energy significantly alters the landscape during its different processes (excavation to waste disposal) and (b) land use has substantial impacts on energy and its efficient use. Researchers reviewed academic articles, books, and institutional reports and made them in an understandable manner in the aspects of land use and energy connection for both the effects of the source and its associated infrastructure on land use and the impacts of human use of land on energy efficiency.

3.1 Impacts of Energy on Land Use

Energy has been considered as one of the most crucial determinants for smooth economic development and people's livelihoods. The per capita energy consumption rate is a basic indicator for determining the economic modernization of a country. Hence, it is well said that countries are more developed when per capita energy consumption is higher. Fossil fuels are a type of energy that has been around for a long time and is still frequently used. People are, however, shifting away from fossil fuels and toward nuclear and renewable energy in order to achieve greater energy efficiency. These energies' production, transmission, and distribution processes have a significant impact on land use [21].

3.1.1 Fossil Fuels and Nuclear Energy

Fossil fuels are forms of organic carbon formed beneath the earth's surface due to excessive heat and pressure of the earth's crust. The most available and easy-to-use fossil fuels are coal, oil, and natural gas. Around 70%-80% of global energy comes from these non-renewable sources. Global output of these fuels grew by almost 67.5 percent in 2019 compared to 1990 [22]. On the other hand, the use of nuclear reactions to generate energy is known as nuclear power. In 2018, nuclear energy produced around 10% of the world's electricity [23]. Fossil fuels such as coal mining, oil and natural gas extraction, and nuclear power generation all have significant impacts on land use in the production and service sectors [16], [19].

Coal

Land transformation occurs both directly and indirectly during the different stages of the coal-fuel cycle. On one hand, coal mines alter land use directly by destroying top soil and cleaning vegetation. On the other hand, as fuel for power plant operations and associated infrastructure, waste indirectly affects land use. Mining excavation, mining methods (surface/underground), coal extraction, waste disposal, and other related processes can convert land from one use to another, with numerous environmental consequences [16], [19], [24]. Several studies have identified coal mining subsidence as a major human geological disaster in China [25], [26], India [27], Greece [28], Korea [29], and elsewhere. Scholars argue that land subsidence causes damage to cultivable land, forest areas, urban neighborhoods, and the overall landscape ecology nearby the mining area. Direct and indirect land use transformation, for example, occurred at and/or near the Barapukuria coal mine in Bangladesh [30].

Coal-fired power stations are established due to the abundance and effectiveness of coal for producing electricity. Hence, coal as fuel indirectly alters the land uses. It is estimated that 6–33 m2/GWh of land transformation required for the entire operation including powerhouse, switchyard, coal storage, stack, walkways, cooling towers etc. of a 1000 MW coal-fired power plant [31]. Coal-fired power plants produce almost 10 Gt of carbon dioxide per year (IEA, 2018), identified as the single most contributor of global greenhouse gas emission in 2018 [32].

Another indirect effect of coal-mining is related to its fuel for mining operation. Wood usage for mine operation that accounts for huge land transformation by both deforestation and afforestation process [31]. Indirect forest losses have been identified almost five times more due to coal mining than direct land use change in Appalachia [33]. It is also examined that about 40% of fly ash and bottom ash are deposited in land or mine filling (indirect effect) in Europe [34] which have several negative effects including contamination in the groundwater and disruption of aquatic systems [35], [36].

Natural Gas and Oil Extraction

The technologies used in extracting natural gas and oil have significant indirect and direct effects on land utilization. Natural gas is extracted from deep wells using fracking methods. In this method, water, sand, and chemicals are injected into the deep well, which makes cracks in the rock layer and withdraws natural gas through the cracks to fill up the well. Although a small amount of land is required for deep wells, usually 28–36 square meters [37], [38], but provision of infrastructure and creation of a vehicle network is needed to maintain the supply chain, supply raw materials to the gas fields, for example, sand for fracking, and supply gas to the potential users [39], [40]. Both technologies (creation of deep wells) and facilities (creation of infrastructure and vehicle networks) have the potential to transform land use patterns in the associated areas [40]–[42]. In addition, injecting wastewater into the wells poses some risk of seismic activity, which may cause land use alteration, but the seismic risk related to injecting wastewater is much smaller than the carbon capture and storage systems have [40], [43].

Oil and gas exploration and exploitation have been causing significant impacts on land use and cover change. For example, about 59,078 sq.km of bare land was converted between 2001 and 2008 to other uses, including oil and gas infrastructure, associated settlement of the newly migrated population due to employment in the industries, agriculture to meet the demand for additional foodstuffs, vegetation increased by afforestation projects etc. in the oil and gas production community of Kwale in Delta State of Nigeria [44], [45].

Furthermore, oil development has other negative consequences, including contamination of water, air, and land; health effects; and road wear and tear. The main concerns are that restoring land from oil activities takes a very long time and that the removed forest area may not recover when the operations are decommissioned [46]. The boreal forest in Canada, for example, is changing as a consequence of oil and gas exploration, transportation, and human settlement expansion. However, oil infrastructure expansion had a greater impact on forests than on water, farming land, or barren land. From 1975 to 2017, they discovered 0.234% deforestation in north-eastern British Columbia [47].

Nuclear Energy

Land is required in the different phases of nuclear power generation, such as mining ore, establishing power stations, management, transportation, and waste disposal [48], [49]. A nuclear power station with a 1000-Megawatt electrical power output requires approximately 330000 tons of uranium ore (0.1% uranium oxide) per year [48]. These amounts of ore can be obtained from underground, surface, or solution mining based on the geological setting of the neighborhood [49]. Approximately 7 ha of land is required to be ore mined to produce 1000-Megawatt electrical power for one year. Land transformation is higher in the case of nuclear power production than coal-fired energy in the USA [31]. In addition, a large buffer area is needed for transporting fuel and waste. The areas are isolated and free from usual development but are being used as wildlife habitats through biodiversity and conservation programs by many nuclear energy operators. Moreover, reprocessing of spent fuel needs further land transformation through establishing transportation systems, operation of reprocessing plants, etc. [40], [48].

3.1.2 Renewable Energy

The decision makers around the world are well aware of our limitations regarding the fossil fuels we have. In addition, oil price fluctuations, increasing changes in climatic conditions and their associated impacts on the world economy have motivated many countries in the world to produce renewable energy both on a small and large scale [16]. Renewable energy is the source of energy that is naturally replenishing and virtually inexhaustible in duration. The energy is acquired from naturally regenerated sources over a human timespan. The most common renewable energy sources are wind energy, solar energy, biomass, hydropower, and deriving energy from waste, etc. These renewable energy sources have significant implications for natural landscape change.

Wind Energy

Wind energy is becoming more familiar as a non-conventional source of energy in many parts of the world. China has the highest installed wind capacity, 221 gigawatts (GW), and the largest wind farm, 7965 megawatts (MW), in the world. The United States is the second largest wind capacity country (96.4 GW), while Germany (59.3 GW) is the third largest. Besides, with 35 GW of wind capacity, India's position is fourth, followed by

Spain (23 GW) and the United Kingdom (20.7 GW) [50]. Agricultural land, livestock grazing, fallow land, etc. are the most compatible land uses for wind energy production because of height and noise issues for establishing wind turbines. Situated in residential or commercial areas, wind turbines are not feasible because adjacent buildings impede the wind on one hand. On the other hand, the noise created due to turbines crosses the recommended noise level (25–40 dB at night, with 10 dB higher for daytime) of the International Standards Organization (ISO). The noise created by wind turbines may vary depending on the power capacity and types of turbines used, as well as available wind speed. The usual range of noise created by wind turbines is 96-108 dB [51]. Therefore, establishing wind turbines needs to change the present land use of agricultural, livestock grazing, and fallow land. Although these changes happen on a small scale, they have significant impacts. In addition, establishing infrastructure for the construction of wind turbines, operation and maintenance, and energy supply systems needs alteration of land uses in the production and service areas [52].

Solar Energy

The demand and use of solar energy have been increasing around the world using two popular methods, i.e., photovoltaic (PV) and concentrated solar power (CSP) systems. In 2015, the total capacity of solar-powered electricity reached 227 gigatons (GWe), accounting for about 1% of global electricity production. PV farms and CSP are large-scale centralized methods of solar energy production that require a huge volume of insolation as well as land use concern. The National Renewable Energy Laboratory (NREL) reported that the average required land area (direct use) for producing 1 MW of electricity in the United States is about 7.3 acres [40]. About 114–261 square meters of land are usually needed depending on available insolation to fulfil a person's energy demands using PV methods [53]. Land use changes (through forest clearance, construction activities, etc.) for solar energy production are observed at different rates in many countries like the United States, China, etc., which have several potential effects on soil erosion [40].

Biomass

Biomass is considered the fourth largest source of energy while the first, second, and third sources are oil, coal, and natural gas, respectively. It uses about 6.41% of total global energy consumption [54]. It is the largest source of renewable energy that can be produced from different sources of raw materials such as agricultural crops, forestry and wood processing residues, algae, household wastes, industrial wet wastes, etc. Biomass energy, such as biogas and biofuel, can be used for cooking, heating, and electricity generation, as well as transportation fuel [55]–[57]. Like other developing countries in South and Southeast Asia, biomass energy is being used as the main source of household energy in Bangladesh [58]. Global demand for biomass energy has doubled in the last four decades and is still increasing [59]. Although only 0.5% to 1.7% of agricultural land is currently used to grow biofuel raw materials, there is significant potential for small-scale and large-scale production [60]. Biomass production is heavily reliant on available cultural land and land use policies, which may increase land transformation [55], [60]–[62]. The effect of biomass on land use is largely due to the cultivation and processing of feedstock, as well as transporting fuel to the power plant. For biomass energy production to work, there needs to be a lot of planning over a long period of time that takes into account competing uses of land and resources [63].

Waste Energy

The water-to-energy (WTE) process has a strong significance for land use alteration. Agricultural or commercial uses of land can be transformed into solid waste disposal sites in order to generate utility and industrial fuel [64]. According to the origin of waste, solid waste can be categorized as (a) municipal solid waste (MSW) includes food-kitchen-green waste, paper waste, product packaging waste, appliance waste, etc.; (b) industrial solid waste (ISW) includes inert industrial waste (chemically or biologically non-reactive) and non-hazardous waste; and (c) healthcare solid waste (HSW), also called solid medical waste (SMW), includes plastic discarded gloves, syringes, bandages, human or animal tissues, clothes, etc. [65]. However, the magnitude of economic or agricultural losses caused by solid waste dumping varies by location, but in most cases, all biodiversity is destroyed in such territory [64]. Particularly, biodiesel generation from municipal solid waste requires available land surface, ignoring food feedstocks that contribute to global land-use change [66].

Hydropower

Hydropower is the most abundant form of renewable energy, accounting for more than 70% of all green energy and more than 16% of global electricity supply from across all energy sources [40]. In contrast to electricity derived from fossil fuels, increasing hydropower energy output has the potential to reduce greenhouse gas emissions [67]. Hydropower is often touted as a low-cost, low-carbon, advanced technology for satisfying growing energy needs and boosting economic growth [68]. River basin management and reservoir creation for establishing a hydropower plant as well as its associated economic activities may trigger the changing nature of social status and economic well-being as a result of changes in land use and land cover (LULC) and hydrologic patterns in the water basin area. In addition, a hydropower project can contribute to increased urbanization through reducing flood risk and improving development activities [69]. And, of course, urbanization has been one of the leading causes of land use change in recent decades. A large-scale hydropower plant includes the construction of structures such as roads, dams, culverts, tunnels, power station infrastructure, and electricity power grids, leading to the clearing of forest and the relocation of human settlements. In addition, the reservoir's inundation on land could kill ecosystems, destroy infrastructure and settlements, harm livelihoods, etc. [70]. The World Commission on Dams reported that about 40-80 million people were displaced due to the socio-economic consequences of dam establishment activities [71]. Later, research on "land use and renewable energy planning'' estimated that indirect deforestation rises between 11.3% and 59% and land use for agriculture increases between 7% and 50% due to hydropower development in any given site for any given year [69].

3.2 Impacts of Land Use on Energy Efficiency

Isolated land use patterns make housing scattered, sparse population densities, average distance traveled for commuting or personal trips, etc. are directly related to increasing vehicle miles traveled [72]. Vehicle miles traveled or VMT is a performance measure widely used in land use and transportation planning with a view to sufficient energy use. It is defined by measuring the total amount of distance traveled by all vehicles in a spatial unit over a fixed period of time, usually one year. VMT is considered as a crucial proxy data for identifying vehicle emissions, energy consumption, etc. [73]–[75]. Energy efficiency (EE), or efficient energy use, is basically defined as using less energy to carry out similar work, and in this way, energy waste can be eliminated. The main concern of EE is to reduce the required amount of energy for producing goods and services. The most efficient way of achieving energy efficiency in the built environment can be obtained through means of land use planning with a view to lowering energy requirements and consumption is by reducing VMT [20], [76]. Sustainable development and energy conservation can be achieved through reducing vehicle miles travelled using a variety of methods, including mixed-use development, urban block development, and encouraging transport-oriented development. In addition, establishing a combined heat and power system, ensuring available green spaces, and energy-supporting land use policies can unlock energy efficiency and ensure sustainable development.

3.2.1 Mixed or Blended Land Use Development

Mixed or blended land use development in the sense of urban development combines at least two distinct types of compatible land uses, such as residential-commercial, residential-commercial-institutional, etc., into one space. It may be in the same building or in close proximity to each other. To some extent, the functions of these blended land uses are physically and functionally integrated [15], [17], [77]. For instance, mixed use development can be vertical where a single building could include a business on the first floor and residential uses on the upper floors, or can be horizontal where a range of different structures on the same site each perform a definite objective, such as a neighborhood area that has housing buildings, office buildings, a playground, a park, a shop, and other facilities (Figure-1). Mixed land use development increases the neighborhood's liveliness and makes the urban environment more attractive. In order to reduce energy demand for motorized travel, average travel distances (commuting or personal trips), and promote walking and other non-motorized travel, mixed land use development is more realistic than monofunctional neighborhoods [15], [78].

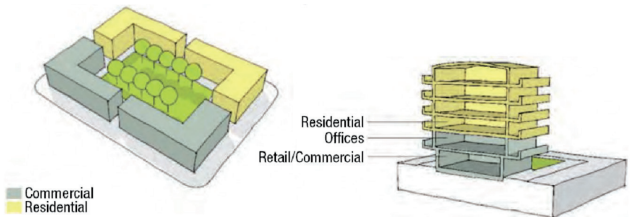

Source: North Shore City [79]

Figure 1: Mixed land use on the Block and Building Scale

One of the earliest cities in North America that adopted mixed-use development policies is Toronto, Canada. City planners started to promote high-density development by blending land uses near to metro stations during the rapid expansion of the city's transit network in the 1960's. In 1980, the regional government of Toronto came up with a plan called Metroplan to promote the use of aligned transit networks. In 1986, the municipal administration took the initial step with a zoning bylaw under the Toronto legal framework that allowed for commercial, residential, and institutional use to be blended and formed a new dimension of land use. The zoning bylaw was revised in 2013 and continues to focus on accommodating a blended land use. Although mixed-or blended-use developments may be found all throughout the city, the majority of Toronto's blended-use zones are concentrated in the city center. City center dominated blended development occurred due to the city's political legacy and developmental history, which has also prioritized combining land uses near transportation networks. The concept of mixed land use in Toronto has been adopted by other Canadian and American cities to effect similar changes[80]–[83].

3.2.2 Urban Block Development

Scholars define an urban block as a part of an urban area that is spatially isolated by road network from the surrounding parts. It is also called the residential cluster encompassed by the road network [84]. There are three types of urban blocks, such as tower blocks, linear blocks, and perimeter blocks. The same amount of floor space could be arranged in towers, linear, and perimeter blocks, but there is a need to control its height. It is estimated that the same result can be achieved in a fifteen-story tower, five-story linear, and three-story perimeter block [85]. There is no fixed size for an urban block, it may vary across the cities around the world. The appropriate extent of a block is up to 120 m considering walkable, active, and livable urban space, but sometimes it may be accepted up to 500 m in high-rise urban areas. In Tokyo-Japan, the size of a typical urban block is 50 m wide, while it is 70-100 m in Vienna or Paris, and 100-120 m in New York and Washington D.C. Urban blocks represent mixed uses and public shops exist on the ground floor, usually in a linear pattern and connected with the road network [17]. Hence, energy savings can be achieved through decreasing energy demand for motorized travel [78].

3.2.3 Transit Oriented Development

The Intergovernmental Panel on Climate Change stated that energy generation and consumption are the key contributors that emit almost two-thirds of greenhouse gas emissions. Cities, particularly their transport systems and household requirements (heating and cooling), are the dominant sources of energy consumption [86]. It is estimated that world energy demand will rise by about 1.3% yearly up to 2040 [87]. Transit-oriented development (TOD) can contribute to reducing a certain amount of greenhouse gas emissions from urban areas. TOD is a tool for urban land use and transportation planning that focuses on mixed-use development within walking distance of transit stops in order to maximize transportation service efficiency [88]–[90]. The distance between origin and destination is a key factor in TOD that influences whether users use transit or not. Many scholars identify that the standard walking distance is 10 minutes from a house, business, or leisure spot to public transport [88], [91]. However, this distance may vary depending on the location and user specific needs.

3.2.4 Combined Heat and Power (CHP)

A country can achieve energy efficiency by introducing and incorporating combined heat and power (CHP) systems at an individual and/or district level. CHP is a system that makes both heat and electricity in a single step [20]. Combined heat and power (CHP) at district level, usually called district heating with combined heat and power (CHP-DH), is a system or process of generating heat at a central level and distributing it to the users' premises through insulated pipes [92]. The actual benefit of CHP-DH, on the other hand, is greater in mixed-use development than in single-use neighborhoods [20], [76]. However, CHP at an individual level also provides an outstanding opportunity to supply heat and power to many buildings, like hotels, educational institutions, medical centers, residential houses, etc.

3.2.5 Green Spaces

Most urban areas are considered the centers of heat generation and are commonly called "urban heat islands" [93] They largely depend on solar insolation, wind speed, cloud cover, humidity, vegetation coverage, construction materials, etc. [94], [95]. Urban heat islands consume vast amounts of cooling energy during the summer season [96]. Sufficient green space in urban areas reduces air temperature on both the horizontal [97] and vertical [96] scales, as well as cooling energy requirements within the urban area and its periphery [17], [94]–[97]. Some scholars explain green spaces as the "natural air conditioner" that can reduce building energy [98], [99] and create barriers to release carbon dioxide, nitrogen dioxide, and ozone gases into the air [100].

3.2.6 Energy Support Land Use Plan and Policies

Land-use planning is "the systematic assessment of land and water potential, alternatives for land use, and economic and social conditions in order to select and adopt the best land-use options" [101]. Land use planning and regulations are public policy exercises that designate and regulate land use in terms of enhancing the environmental, financial, and sociocultural efficiency or well-being of a community. These regulations are also involved in achieving energy efficiency or diminishing marginal energy demand. Many scholars [20], [102], [103] identified land use policies as the root cause of land use change. Land use policies can attain energy conservation by incorporating several sections regarding mixed use development, urban block formation, transport-oriented structural development, establishment of combined heat and power systems, green field development, improvement of mass transport, walking, cycling access, etc. [17].

4. CONCLUSIONS

Land use is the human utilization of land, which is considered the modification, alteration, and management of the physical environment into built environments such as settlements, agriculture, transportation, industry, recreation, and open space. The changing pattern of land use is a major concern for the improvement of the healthy well-being of human society. Energy has been considered as the central determinant for smooth economic development and people's livelihoods. The nexus between land use and energy can be discussed as the impacts of energy on land usage and, conversely, the impacts of land use on energy. It is recognized that direct and indirect land use changes occur during the different stages of extraction, deposition, and transportation of fossil fuels and uranium ore. Mining for fossil fuels and uranium ore has a direct impact on land usage by clearing vegetation and destroying top soil. Furthermore, supplying fuel for mining operations, establishing associated infrastructure, and disposing of waste all have an indirect impact on the land uses of the associated areas. Moreover, generating renewable energy also has several direct and indirect impacts on land usage. The installation of wind turbines necessitates a direct change in the current land use of agricultural, animal grazing, and fallow land. In addition, creating infrastructure for wind turbine construction, operation, and maintenance, as well as an energy supply system, requires land use changes in the production and service areas. Furthermore, the effects of biomass on land usage are primarily attributable to feedstock cultivation and processing as well as fuel transportation to power plants. Likewise, the production of biodiesel from municipal solid waste requires available land surface, ignoring food feedstocks, which contribute to global land-use change. In a similar way, the building of highways, dams, culverts, tunnels, power station infrastructure, and energy transmission networks for large-scale hydropower plants leads to the destruction of forests and the relocation of people.

This research found blended land use development as the most efficient approach to achieve energy efficiency through land use planning. This form of development, which is more practical than a monofunctional neighborhood, mixes at least two different types of compatible land uses to minimize energy demand for motorized travel, average commute or personal trip distances, and encourage non-motorized modes of transportation like walking. Furthermore, urban block and transit-oriented development can significantly lower the energy demand for vehicle trips. Moreover, an integrated heat and power system, green space in the neighborhood, as well as energy-supporting land use plans and regulations, may help to achieve energy efficiency and ensure long-term development.

Funding: ERASMUS+ PROGRAMME OF THE EUROPEAN UNION, grant number 598746-EPP-1-2018-LT-EPPKA2-CBHE-JP.

REFERENCES

[1] G. N. T. Hasnat, M. A. Siddik, and A. K. M. M. Zaman, "Land Use Changing Pattern and Challenges for Agricultural Activities: A Study on Dumki Upazila, Patuakhali," *J. Patuakhali Sci. and Tech. Uni*, vol. 1 & 2, pp. 67–76, 2018.

[2] P. Kenrick and P. R. Crane, "The origin and early evolution of plants on land," *Nature*, vol. 389, no. 6646, pp. 33–39, 1997, doi: 10.1038/37918.

[3] J. R. Anderson, E. E. Hardy, J. T. Roach, and R. E. Witmer, "A land use and land cover classification system for use with remote sensor data," Washington, 1976. doi: 10.3133/PP964.

[4] Md. A. Siddik, Md. A. Rahman, and Md. Moniruzzaman, "Causes and Consequences of Land Disputes in the Coastal Area of Bangladesh," *Eastern Geographer*, vol. 14, no. 2, pp. 7–15, 2018.

[5] N. Farah, I. A. Khan, A. A. Maan, B. Shahbaz, and J. M. Cheema, "Driving Factors of Agricultural Land Conversion at Rural-Urban Interface in Punjab, Pakistan," *Journal of Agricultural Research*, vol. 57, no. 1, pp. 55–62, 2019.

[6] H. Briassoulis, "Factors Influencing Land-Use and Land-Cover Change," in *Land Use, Land Cover and Soil Science*, vol. I, W. H. Verheye, Ed. 2009.

[7] E. F. Lambin, H. J. Geist, and E. Lepers, "Dynamics of land-use and land-cover change in tropical regions," *Annual Review of Environment and Resources*, vol. 28, pp. 205–241, Nov. 2003, doi: 10.1146/annurev.energy.28.050302.105459.

[8] H. Azadi, P. Ho, and L. Hasfiati, "Agricultural land conversion drivers: A comparison between less developed, developing and developed countries," *Land Degradation & Development*, vol. 22, no. 6, pp. 596–604, Nov. 2011, doi: 10.1002/ldr.1037.

[9] H. Thuc Vien, L. T. Ward, T. D. District, and H. Chi, "The linkage between land reform and land use changes: A case of Vietnam," *Journal of Soil Science and Environmental Management*, vol. 2, no. 3, pp. 88–96, Mar. 2011.

[10] N. Nzunda, P. Munishi, G. Soka, and J. Monjare, "Influence of socio-economic factors on land use and vegetation cover changes in and around Kagoma forest reserve in Tanzania," *Ethiopian Journal of Environmental Studies and Management*, vol. 6, no. 5, pp. 480–488, Aug. 2013, doi: 10.4314/ejesm.v6i5.5.

[11] M. Ghatak and D. Mookherjee, "Land acquisition for industrialization and compensation of displaced farmers," *Journal of Development Economics*, vol. 110, pp. 303–312, Sep. 2014, doi: 10.1016/j.jdeveco.2013.01.001.

[12] H. Huq, "Solar energy fuels for sustainable livelihoods: Case study of southwest coastal region of Bangladesh," *Geography, Environment, Sustainability*, vol. 11, no. 4, pp. 132–143, Jan. 2018, doi: 10.24057/2071-9388-2018-11-4-132-143.

[13] V. Brkić, "Energy Decarbonisation and Primary Energy in the 21st Century," *Journal of Energy - Energija*, vol. 70, no. 2, pp. 11–16, Jun. 2021, doi: 10.37798/20217028.

[14] M. Krpan and I. Kuzle, "The mathematical model of a wind power plant and a gas power plant," *Journal of Energy - Energija*, vol. 66, no. 1–4, pp. 69–86, Jun. 2022, doi: 10.37798/2017661-491.

[15] C. Keeley and B. D. Frost, "Land Use and Energy: Connecting the Dots to Enhance Communities Why Do Land Use and Energy Matter? Who Makes Decisions about Land Use and Energy?," 2014. [Online]. Available: http://www.mrsc.org/subjects/planning/lu/mixedusedev.aspx.

[16] N. Kaza and M. P. Curtis, "The Land Use Energy Connection," *Journal of Planning Literature*, vol. 29, no. 4, pp. 355–369, Nov. 2014, doi: 10.1177/0885412214542049.

[17] World Bank, "Planning Energy Efficient and Livable Cities. Mayoral Guidance Note #6, ESMAP," 2014. Accessed: Apr. 13, 2021. [Online]. Available: https://www.esmap.org/node/55381.

[18] United Nations, "World Urbanization Prospects 2018 Highlights," 2019. Accessed: Apr. 13, 2021. [Online]. Available: https://population.un.org/wup/Publications/Files/WUP2018-Highlights.pdf.

[19] NEED, *Intermediate Energy Infobook*. Manassas: National Energy Education Development, 2019.

[20] J. R. Nolon, "Land Use for Energy Conservation and Sustainable Development: A New Path Toward Climate Change Mitigation," *SSRN Electronic Journal*, Jan. 2012, doi: 10.2139/ssrn.1951905.

[21] A. Babatunde Onakoya, A. Olatunde Onakoya, O. Adejuwon Jimi -Salami, and B. Omoniyi Odedairo, "Energy Consumption and Nigerian Economic Growth: An Empirical Analysis," *European Scientific Journal*, vol. 9, no. 4, pp. 1857–7881, Feb. 2013.

[22] M. A. Siddik, M. T. Islam, A. K. M. M. Zaman, and M. M. Hasan, "Current Status and Correlation of Fossil Fuels Consumption and Greenhouse Gas Emissions," *International Journal of Energy, Environment and Economics*, vol. 28, no. 2, pp. 103–118, 2021, Accessed: Jun. 25, 2022. [Online]. Available: https://novapublishers.com/shop/volume-28-issue-2-international-journal-of-energy-environment-and-economics/

[23] World Nuclear Association, "Nuclear Power in the World Today ," 2021. https://www.world-nuclear.org/information-library/current-and-future-generation/nuclear-power-in-the-world-today.aspx (accessed May 23, 2021).

[24] F. G. Bell, T. R. Stacey, and D. D. Genske, "Mining subsidence and its effect in the environment: Some differing examples," *Environmental Geology*, vol. 40, no. 1–2, pp. 135–152, 2000, doi: 10.1007/s002540000140.

[25] W. Quanyuan *et al.*, "Impacts of coal mining subsidence on the surface landscape in Longkou city, Shandong Province of China," *Environmental Earth Sciences*, vol. 59, no. 4, pp. 783–791, Feb. 2009, doi: 10.1007/s12665-009-0074-9.

[26] K. Ma, Y. Zhang, M. Ruan, J. Guo, and T. Chai, "Land Subsidence in a Coal Mining Area Reduced Soil Fertility and Led to Soil Degradation in Arid and Semi-Arid Regions," *International Journal of Environmental Research and Public Health*, vol. 16, no. 20, p. 3929, Oct. 2019, doi: 10.3390/ijerph16203929.

[27] S. Rehman *et al.*, "Assessing subsidence susceptibility to coal mining using frequency ratio, statistical index and Mamdani fuzzy models: evidence from Raniganj coalfield, India," *Environmental Earth Sciences*, vol. 79, no. 16, pp. 1–18, Aug. 2020, doi: 10.1007/s12665-020-09119-8.

[28] C. Loupasakis, V. Angelitsa, D. Rozos, and N. Spanou, "Mining geohazards-land subsidence caused by the dewatering of opencast coal mines: The case study of the Amyntaio coal mine, Florina, Greece," *Natural Hazards*, vol. 70, no. 1, pp. 675–691, Jan. 2014, doi: 10.1007/s11069-013-0837-1.

[29] J. K. Choi, K. D. Kim, S. Lee, and J. S. Won, "Application of a fuzzy operator to susceptibility estimations of coal mine subsidence in Taebaek City, Korea," *Environmental Earth Sciences*, vol. 59, no. 5, pp. 1009–1022, Jan. 2010, doi: 10.1007/s12665-009-0093-6.

[30] S. Roy, M. M. M. Hoque, D. R. Roy, M. A. S. Shanta, and S. Roy, "Level of mineral elements in soil and plant roots of the adjacent area of Barapukuria coal mine Physico-chemical characterization of soils of some agricultural lands of Patenga thana, Chittagong View project," *Journal of Innovation & Development Strategy (JIDS)*, vol. 7, no. 3, pp. 10–13, 2013.

[31] V. Fthenakis and H. C. Kim, "Land use and electricity generation: A life-cycle analysis," *Renewable and Sustainable Energy Reviews*, vol. 13, no. 6–7, pp. 1465–1474, Aug. 2009, doi: 10.1016/j.rser.2008.09.017.

[32] I. Gençsü et al., "G20 coal subsidies Tracking government support to a fading industry," 2019. Accessed: Apr. 13, 2021. [Online]. Available: https://www.odi.org/sites/odi.org.uk/files/resource-documents/12744.pdf.

[33] J. D. Wickham, K. H. Riitters, T. G. Wade, M. Coan, and C. Homer, "The effect of Appalachian mountaintop mining on interior forest," *Landscape Ecology*, vol. 22, no. 2, pp. 179–187, Feb. 2007, doi: 10.1007/s10980-006-9040-z.

[34] J. Skousen, P. Ziemkiewicz, and J. E. Yang, "Use of coal combustion by-products in mine reclamation:Review of case studies in the usa," *Geosystem Engineering*, vol. 15, no. 1, pp. 71–83, 2012, doi: 10.1080/12269328.2012.676258.

[35] C. L. Carlson and D. C. Adriano, "Environmental Impacts of Coal Combustion Residues," *Journal of Environmental Quality*, vol. 22, no. 2, pp. 227–247, Apr. 1993, doi: 10.2134/jeq1993.00472425002200020002x.

[36] R. J. Haynes, "Reclamation and revegetation of fly ash disposal sites - Challenges and research needs," *Journal of Environmental Management*, vol. 90, no. 1, pp. 43–53, Jan. 2009, doi: 10.1016/j.jenvman.2008.07.003.

[37] NYSDEC, "Revised draft supplemental generic environmental impact statement (SGEIS) on the oil, gas and solution mining regulatory program: Well permit issuance for horizontal drilling and high-volume hydraulic fracturing to develop the Marcellus shale and other low-permeability gas reservoirs," 2009. Accessed: Apr. 13, 2021. [Online]. Available: http://www.dec.ny.gov/energy/75370.html.

[38] R. Smith and T. Ozer, "North Carolina oil and gas study under session law 2011-276," North Carolina, 2012. Accessed: Apr. 13, 2021. [Online]. Available: https://files.nc.gov/ncdeq/Energy Mineral and Land Resources/Energy/documents/Shale Gas/Shale Gas Report Final amend.pdf.

[39] Y. Yang, "A Study of Shale Gas Production and Its Supply Chain," University of Pittsburgh, 2016.

[40] World Energy Council, "World Energy Resources 2016," 2016. [Online]. Available: www.worldenergy.org.

[41] H. Schaffer Boudet and L. Ortolano, "A Tale of Two Sitings: Contentious Politics in Liquefied Natural Gas Facility Siting in California," *Journal of Planning Education and Research*, vol. 30, no. 1, pp. 5–21, Sep. 2010, doi: 10.1177/0739456X10373079.

[42] T. Kumpula, B. C. Forbes, F. Stammler, and N. Meschtyb, "Dynamics of a Coupled System: Multi-Resolution Remote Sensing in Assessing Social-Ecological Responses during 25 Years of Gas Field Development in Arctic Russia," *Remote Sensing*, vol. 4, no. 4, pp. 1046–1068, Apr. 2012, doi: 10.3390/rs4041046.

[43] National Research Council, *Induced seismicity potential in energy technologies*. National Academies Press, 2013. doi: 10.17226/13355.

[44] S. Matemilola, O. H. Adedeji, and E. C. Enoguanbhor, "Land Use/Land Cover Change in Petroleum-Producing Regions of Nigeria," in *The Political Ecology of Oil and Gas Activities in the Nigerian Aquatic Ecosystem*, P. E. Ndimele, Ed. Elsevier Inc., 2018, pp. 257–276. doi: 10.1016/B978-0-12-809399-3.00017-3.

[45] A. Dami, J. O. Odihi, and H. A. Ayuba, "Assessment of Land use and Land Cover Change in Kwale, Ndokwa-East Local Government Area, Delta State, Nigeria," *Global Journal of Human-Social Science Research*, vol. 14, no. 6, pp. 16–24, 2014.

[46] M. Hebblewhite, "Billion dollar boreal woodland caribou and the biodiversity impacts of the global oil and gas industry," *Biological Conservation*, vol. 206, pp. 102–111, Feb. 2017, doi: 10.1016/j.biocon.2016.12.014.

[47] J. Oduro Appiah, C. Opio, and S. Donnelly, "Measuring forest change patterns from oil and gas land use dynamics in northeastern British Columbia, 1975 to 2017," *Environmental Monitoring and Assessment*, vol. 192, no. 1, pp. 1–18, Jan. 2020, doi: 10.1007/s10661-019-7958-2.

[48] D. Green, "Land use and nuclear energy," *Land Use Policy*, vol. 4, no. 2, pp. 90–95, Apr. 1987, doi: 10.1016/0264-8377(87)90042-1.

[49] E. E. El-Hinnawi, "Review of the environmental impact of nuclear energy." 1977, Accessed: Apr. 12, 2021. [Online]. Available: http://inis.iaea.org/Search/search.aspx?orig_q=RN:8303221.

[50] ETEnergyWorld, "Wind energy capacity: World's top 10 countries in wind energy capacity, Energy News, ET EnergyWorld," 2019.

[51] M. Bastasch, J. Van Dam, B. Sonder-

gaard, and A. Rogers, “Wind Turbine Noise-an Overview,” *Canadian Acoustics*, vol. 34, no. 2, pp. 7–15, Jun. 2006.

[52] A. L. Drewitt and R. H. W. Langston, “Assessing the impacts of wind farms on birds,” *International Journal of Avian Science*, vol. 148, no. SUPPL. 1, pp. 29–42, Mar. 2006, doi: 10.1111/j.1474-919X.2006.00516.x.

[53] P. Denholm and R. M. Margolis, “Land-use requirements and the per-capita solar footprint for photovoltaic generation in the United States,” *Energy Policy*, vol. 36, no. 9, pp. 3531–3543, Sep. 2008, doi: 10.1016/j.enpol.2008.05.035.

[54] H. Ritchie, “Energy mix - Our World in Data,” *Our World in Data*, 2019. https://ourworldindata.org/energy-mix (accessed Apr. 14, 2021).

[55] S. Nonhebel, “Renewable energy and food supply: Will there be enough land?,” *Renewable and Sustainable Energy Reviews*, vol. 9, no. 2, pp. 191–201, Apr. 2005, doi: 10.1016/j.rser.2004.02.003.

[56] N. E. Korres, A. Singh, A.-S. Nizami, and J. D. Murphy, “Is grass biomethane a sustainable transport biofuel?,” *Biofuels, Bioproducts and Biorefining*, vol. 4, no. 3, pp. 310–325, May 2010, doi: 10.1002/bbb.228.

[57] A. Prochnow, M. Heiermann, M. Plöchl, T. Amon, and P. J. Hobbs, “Bioenergy from permanent grassland - A review: 2. Combustion,” *Bioresource Technology*, vol. 100, no. 21, pp. 4945–4954, Nov. 2009, doi: 10.1016/j.biortech.2009.05.069.

[58] M. K. Hassan, P. Halder, P. Pelkonen, and A. Pappinen, “Rural households’ preferences and attitudes towards biomass fuels - results from a comprehensive field survey in Bangladesh,” *Energy, Sustainability and Society*, vol. 3, no. 1, pp. 1–14, Dec. 2013, doi: 10.1186/2192-0567-3-24.

[59] L. Singh and Z. A. Wahid, “Methods for enhancing bio-hydrogen production from biological process: A review,” *Journal of Industrial and Engineering Chemistry*, vol. 21, pp. 70–80, Jan. 2015, doi: 10.1016/j.jiec.2014.05.035.

[60] A. Faaij, “Developments in international bio-energy markets and trade,” *Biomass and Bioenergy*, vol. 32, no. 8, pp. 657–659, Aug. 2008, doi: 10.1016/j.biombioe.2008.02.008.

[61] M. Hoogwijk, A. Faaij, R. Van Den Broek, G. Berndes, D. Gielen, and W. Turkenburg, “Exploration of the ranges of the global potential of biomass for energy,” *Biomass and Bioenergy*, vol. 25, no. 2, pp. 119–133, Aug. 2003, doi: 10.1016/S0961-9534(02)00191-5.

[62] D. J. A. Johansson and C. Azar, “A scenario based analysis of land competition between food and bioenergy production in the US,” *Climatic Change*, vol. 82, no. 3–4, pp. 267–291, Jun. 2007, doi: 10.1007/s10584-006-9208-1.

[63] M. P. Curran and S. W. Howes, “Soil disturbance concerns regarding the use of forest biomass as a source of energy: Examples from Pacific Northwestern North America,” *Biomass and Bioenergy*, vol. 35, no. 11, pp. 4547–4556, Nov. 2011, doi: 10.1016/j.biombioe.2011.09.017.

[64] K. E. Robeck et al., “Land Use and Energy,” 1980. Accessed: Apr. 18, 2021. [Online]. Available: https://inis.iaea.org/collection/NCLCollectionStore/_Public/12/641/12641386.pdf.

[65] T. A. Hamad, A. A. Agll, Y. M. Hamad, and J. W. Sheffield, “Solid waste as renewable source of energy: Current and future possibility in Libya,” *Case Studies in Thermal Engineering*, vol. 4, pp. 144–152, Nov. 2014, doi: 10.1016/j.csite.2014.09.004.

[66] T. Searchinger *et al.*, “Use of U.S. croplands for biofuels increases greenhouse gases through emissions from land-use change,” *Science (1979)*, vol. 319, no. 5867, pp. 1238–1240, Feb. 2008, doi: 10.1126/science.1151861.

[67] M. Dorber, R. May, and F. Verones, “Modeling Net Land Occupation of Hydropower Reservoirs in Norway for Use in Life Cycle Assessment,” *Environmental Science and Technology*, vol. 52, no. 4, pp. 2375–2384, Feb. 2018, doi: 10.1021/acs.est.7b05125.

[68] V. Djelić, I. Kern, Z. Peršin, and M. Ocepek, “Trends in Hydropower,” *Journal of Energy - Energija*, vol. 70, no. 2, pp. 17–23, Jun. 2021, doi: 10.37798/202170255.

[69] G. C. Wu, “Land Use in Renewable Energy Planning,” University of California, Berkeley, 2018.

[70] C. S. Kaunda, C. Z. Kimambo, and T. K. Nielsen, “Hydropower in the Context of Sustainable Energy Supply: A Review of Technologies and Challenges,” *ISRN Renewable Energy*, vol. 2012, pp. 1–15, Dec. 2012, doi: 10.5402/2012/730631.

[71] World Commission on Dams, “Dams and development: A new framework for decision-making. Overview of the report by the World Commission on Dams,” London, 2001. Accessed: Apr. 18, 2021. [Online]. Available: https://pubs.iied.org/sites/default/files/pdfs/migrate/9126IIED.pdf.

[72] A. W. Sadek, Q. Wang, P. Su, and A. Tracy, “Reducing Vehicle Miles Traveled Through Smart Land-Use Design,” Dec. 2011.

[73] D. Kim and J. Lee, “Application of neural network model to vehicle emissions,” *International Journal of Urban Sciences*, vol. 14, no. 3, pp. 264–275, 2010, doi: 10.1080/12265934.2010.9693684.

[74] A. T. Moore, S. R. Staley, and R. W. Poole, “The role of VMT reduction in meeting climate change policy goals,” *Transportation Research Part A: Policy and Practice*, vol. 44, no. 8, pp. 565–574, Oct. 2010, doi: 10.1016/j.tra.2010.03.012.

[75] L. Zhang, X. He, Y. Lu, C. Krause, and N. Ferrari, “Are we successful in reducing vehicle miles traveled in air quality nonattainment areas?,” *Transportation Research Part A: Policy and Practice*, vol. 66, no. 1, pp. 280–291, Aug. 2014, doi: 10.1016/j.tra.2014.05.016.

[76] S. E. Owens, “Land-use planning for energy efficiency,” *Applied Energy*, vol. 43, no. 1–3, pp. 81–114, Jan. 1992, doi: 10.1016/0306-2619(92)90075-M.

[77] R. Raman and U. K. Roy, “Taxonomy of urban mixed land use planning,” *Land Use Policy*, vol. 88, p. 104102, Nov. 2019, doi: 10.1016/j.landusepol.2019.104102.

[78] R. Farjam and S. M. Hossieni Motlaq, “Does urban mixed use development approach explain spatial analysis of inner city decay?,” *Journal of Urban Management*, vol. 8, no. 2, pp. 245–260, Aug. 2019, doi: 10.1016/j.jum.2019.01.003.

[79] North Shore City, “Mixed Use Town Center Good Solutions Guide for Mixed Use Development in Town Centers,” 2005. Accessed: Apr. 13, 2021. [Online]. Available: http://imakelma.com/books/98/mixed-use-guide-2005-sm.pdf.

[80] P. Filion, “The Urban Growth Centres Strategy in the Greater Golden Horseshoe,” 2007. Accessed: Apr. 12, 2021. [Online]. Available: https://neptis.org/sites/default/files/nodes_and_corridors/filion_electronic_report_20070528.pdf.

[81] S. Darchen, “The Creative City and the Redevelopment of the Toronto Entertainment District: A BIA-Led Regeneration Process,” *International Planning Studies*, vol. 18, no. 2, pp. 188–203, May 2013, doi: 10.1080/13563475.2013.774147.

[82] City of Toronto, “By-law 569-2013 Zoning By-law for the City of Toronto,” 2013. Accessed: Apr. 13, 2021. [Online]. Available: http://www.toronto.ca/legdocs/bylaws/2013/law0569-schedule-a-vol1-ch1-800.pdf.

[83] M. Moos, T. Vinodrai, N. Revington, and M. Seasons, “Planning for Mixed Use: Affordable for Whom?,” *Journal of the American Planning Association*, vol. 84, no. 1, pp. 7–20, Jan. 2018, doi: 10.1080/01944363.2017.1406315.

[84] K. Williams, “Designing the City: towards a more sustainable urban form,” *URBAN DESIGN International*, vol. 6, no. 2, pp. 116–117, Jun. 2001, doi: 10.1057/palgrave.udi.9000045.

[85] G. Towers, *Introduction to Urban Housing Design*, 1st ed. Routledge , 2005.

[86] IPCC, “AR5 Climate Change 2014: Mitigation of Climate Change — IPCC,” Geneva, Switzerland, 2014. Accessed: Apr. 13, 2021. [Online]. Available: https://www.ipcc.ch/report/ar5/wg3/.

[87] IEA, “World Energy Outlook 2019 – Analysis,” 2019. Accessed: Apr. 13, 2021. [Online]. Available: https://www.iea.org/reports/world-energy-outlook-2019.

[88] P. Calthorpe, *The next American metropolis : ecology, community, and the American dream*. New York: Princeton Architectural Press, 1993.

[89] A. V. Sohoni, M. Thomas, and K. V. K. Rao, “Application of the concept of transit oriented development to a suburban neighborhood,” in *Transportation Research Procedia*, Jan. 2017, vol. 25, pp. 3220–3232. doi: 10.1016/j.trpro.2017.05.135.

[90] A. Ibraeva, G. H. de A. Correia, C. Silva, and A. P. Antunes, “Transit-oriented development: A review of research achievements and challenges,” *Transportation Research Part A: Policy and Practice*, vol. 132, pp. 110–130, Feb. 2020, doi: 10.1016/j.tra.2019.10.018.

[91] E. Guerra, R. Cervero, and D. Tischler, “Half-Mile Circle: Does It Best Represent Transit Station Catchments? ,” *Transportation Research Record: Journal of the Transportation Research Board*, vol. 2276, no. 1, pp. 101–109, Jan. 2012, doi: 10.3141/2276-12.

[92] S. Kelly and M. Pollitt, “Making Combined Heat and Power District Heating (CHP-DH) Networks in the United Kingdom Economically Viable: A Comparative Approach,” Energy Policy Research Group, Cambridge Judge Business School, University of Cambridge, 2009. Accessed: Apr. 13, 2021. [Online]. Available: https://ideas.repec.org/p/enp/wpaper/eprg0925.html.

[93] G. Grdenić and Ž. Tomšić, “Renewable energy sources and other energy technologies as a measure for mitigating the impact of urban heat islands,” *Journal of Energy - Energija*, vol. 66, no. 1–4, pp. 184–194, Jun. 2022, doi: 10.37798/2017661-4104.

[94] M. Arboit and E. Betman, “Evaluation of the Energy Impact of Green Area Surfaces and Vegetation Cover in Forested Urban Environments with Dry Climates. Case: Mendoza Metropolitan Area, Argentina,” *Procedia Environmental Sciences*, vol. 37, pp. 112–130, Jan. 2017, doi: 10.1016/j.proenv.2017.03.027.

[95] R. Giridharan and R. Emmanuel, “The impact of urban compactness, comfort strategies and energy consumption on tropical urban heat island intensity: A review,” *Sustainable Cities and Society*, vol. 40, pp. 677–687, Jul. 2018, doi: 10.1016/j.scs.2018.01.024.

[96] F. Kong *et al.*, “Energy saving potential of fragmented green spaces due to their temperature regulating ecosystem services in the summer,” *Applied Energy*, vol. 183, pp. 1428–1440, Dec. 2016, doi: 10.1016/j.apenergy.2016.09.070.

[97] L. Shashua-Bar, D. Pearlmutter, and E. Erell, “The influence of trees and grass on outdoor thermal comfort in a hot-arid environment,” *International Journal of Climatology*, vol. 31, no. 10, pp. 1498–1506, Aug. 2011, doi: 10.1002/joc.2177.

[98] T. V. Ca, T. Asaeda, and E. M. Abu, “Reductions in air conditioning energy caused by a nearby park,” *Energy and Buildings*, vol. 29, no. 1, pp. 83–92, Dec. 1998, doi: 10.1016/s0378-7788(98)00032-2.

[99] C. Y. Jim, “Air-conditioning energy consumption due to green roofs with different building thermal insulation,” *Applied Energy*, vol. 128, pp. 49–59, Sep. 2014, doi: 10.1016/j.apenergy.2014.04.055.

[100] D. J. Nowak, J. C. Stevens, S. M. Sisinni, and C. J. Luley, “Effects of Urban Tree Management and Species Selection on Atmospheric Carbon Dioxide,” *Journal of Arboriculture*, vol. 28, no. 3, pp. 113–122, 2002.

[101] FAO, *Guidelines for land-use planning*. Rome, Italy: FAO Development Series No. 1, 1993.

[102] J. van Vliet, A. K. Bregt, D. G. Brown, H. van Delden, S. Heckbert, and P. H. Verburg, “A review of current calibration and validation practices in land-change modeling,” *Environmental Modelling and Software*, vol. 82, pp. 174–182, Aug. 2016, doi: 10.1016/j.envsoft.2016.04.017.

[103] A. M. Hersperger *et al.*, “Urban land-use change: The role of strategic spatial planning,” *Global Environmental Change*, vol. 51, pp. 32–42, Jul. 2018, doi: 10.1016/j.gloenvcha.2018.05.001.

Journal of Energy

VOLUME 70 Number 3 | 2021

journal homepage: http://journalofenergy.com/

Marija Čuljak
University of Zagreb
Faculty of Electrical Engineering and Computing
Unska 3, 10 000 Zagreb, Croatia
Marija.culjak@fer.hr

Mateo Beus
University of Zagreb
Faculty of Electrical Engineering and Computing
Unska 3, 10 000 Zagreb, Croatiam

Hrvoje Pandzic
University of Zagreb
Faculty of Electrical Engineering and Computing
Unska 3, 10 000 Zagreb, Croatia
hrvoje.pandzic@fer.hr

Development of a LabVIEW - Based Data Logging and Monitoring Application for a Photovoltaic Power Plant at FER

SUMMARY

The purpose of this paper is to implement an application in LabVIEW programming language which logs the measurements from photovoltaic (PV) inverters. The application's communication module is connected to the inverters of the PVs via the Modbus TCP/IP protocol and collects the measurements of appropriate process quantities, such as the active power, the total electricity produced, the panel temperature, the insolation, the air temperature, etc. Furthermore, all the collected measurements are saved on a 15-minute basis in separate csv files for each day. Additionally, a graphical user interface (GUI) is developed, where the collected measurements from the PV are displayed. The PV for which the application is developed is located on the roof of the building B of the University of Zagreb Faculty of Electrical Engineering and Computing (FER).

KEY WORDS

photovoltaic inverter, SCADA systems, Modbus TCP/IP protocol, LabVIEW, measurements logging, user interface

1. INTRODUCTION

Technical and scientific challenges of the twenty-first century lay in providing energy to humanity in a safe, sustainable, and clean way [1]. According to this goal, photovoltaic (PV) sources are currently one of the most relevant renewable energy resources (RES), e.g. [2]. PV systems are attractive for electricity generation due to no carbon emissions during operation and easy maintenance, as compared to the other RES. The available solar radiation needed to meet the world's energy requirements is more than sufficient. For these reasons, in the last decade, the PV systems market has experienced a remarkable growth, primarily due to reduced production costs and increased electricity prices [1]. As compared to the above-mentioned benefits, PV also have some limitations, such as dependencies of geographical longitude and latitude, weather forecasting, and limitations in production energy only during the sunny days [3]. Consequently, the supervisory control and monitoring of these systems is especially significant for the optimization of their effectiveness.

This paper presents a detail characterization of performance and dynamic behavior of a PV system using a real-time application developed in LabVIEW. LabVIEW is a graphic programming language that has found its application in many scientific fields and technical engineering. In this paper, the development of an application for collecting, processing, and monitoring the measurements from a PV system is described. The proposed method is a cheaper solution than many commercial SCADA (Supervisory Control and Data Acquisition) systems, which provides reliability and safety by creating a database used for a detailed analysis of the PV system. The developed application and collected measurements are according to the implemented advanced measurement system proposed in [4]. Many applications developed in the LabVIEW for tracking PV systems are shown in the following literature [1], [3], [5], [6], [7].

The remainder of the paper is structured as follows. The second section describes technical characteristics of PV located at the University of Zagreb Faculty of Electrical Engineering and Computing (UNIZG-FER), where the measurements are acquired. In the third section, the Modbus TCP/IP protocol is presented, which is used for the establishing a communication between the PV inverters and the server. A detailed description of the

Marija Čuljak, Mateo Beus, Hrvoje Pandzic, Development of a LabVIEW - Based Data Logging and Monitoring Application for a Photovoltaic Power Plant at FER, Journal of Energy, vol. 70 Number 3 (2021), p. 14–18
https://doi.org/10.37798/2021703133

functionality of the developed application is provided in the fourth chapter, along with a graphical representation of the collected measurements.

2. PV SYSTEM

The intensity of solar radiation in Croatia is among the highest in Europe. For example, the annual sum of global radiation is 1300 kWh/m2 in the northern parts of Croatia and increases up to 1850 kWh/m2 in the southern parts of Croatia [8]. Possible annual electricity production in 1 kWp (PV system capacity; the maximum electrical capacity that a PV cell can give in ideal circumstances: a solar collector facing the sun in a cloudless sky) system ranges from 975 kWh/kW in the northern Croatia up to 1375 kWh/kW in the southern Croatia [8]. The reference electric power that a PV panel produces is defined for an average cell temperature of 25 °C and solar radiation intensity of 1000 W/m². Under these conditions, the PV cell generates maximum power. This value is relevant for producers, but in operating conditions terms, the power of a PV cell depends on the temperature changes and the level of solar irradiation [9].

PV inverter is the main element of any PV system, as it converts direct current of PV modules into alternative current compatible with the network. It simultaneously controls and monitors the entire power plant. The inverter measures voltage, current, frequency and impedance of the network, and is switched off if any of these values deviates from its default value range. This ensures, on the one hand, that the PV modules always operate at maximum power, depending on the irradiation and the temperature. On the other hand, it continuously monitors the electrical network, and is responsible for compliance to various security criteria. In the PV plant at UNIZG-FER, two types of PV inverters are used: Sunny Tripower 10000TL-20, manufactured by SMA [10], and Fronius Symo 12.5-3-M manufactured by Schrack industry [11] .

2.1 Sunny Tripower 10000TL-20

Sunny Tripower 10000TL-20 is a three-phase inverter without a transformer, nominal power of 10 kW and maximum efficiency of 97,6 %. At its input A, there is a Maximum Power Point (MPP) tracker related to the west orientation and has twenty-one modules, while at the input B there is an MPP tracker related to the east orientation and also has twenty-one modules, as shown in Figure 1. In addition to the above, the inverter is equipped with an overcurrent protection of strings, a monitoring system for the network operation, a device for automatic synchronization to the network voltage, a monitoring system for the waveform of the network voltage and protective devices. The expected annual yields obtained by the simulation for the Sunny Tripower 10000TL-20 inverter are around 1065 kWh per installed kilowatt of PV field power [12].

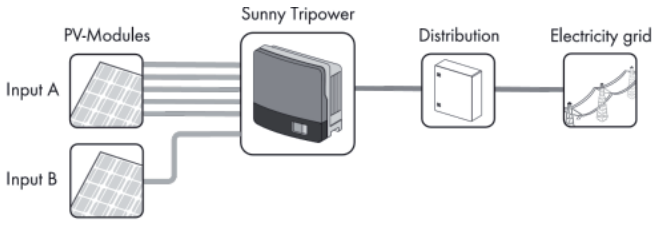

Figure 1. Connecting Sunny Tripower inverter with a PV system [12]

The technical parameters and specification of Sunny Tripower 10000TL-20 are shown in Table 1.

Table 1 Technical parameters of Sunny Tripower 10000TL-20 inverter [12]

Parameter	Value
Max. input (DC) power	13.500 Wp
Max. input (DC) power	1000 V
Input voltage operating range	320 – 800 V
Max. output (AC) power	10000 W
Num. of MPPT units	2
Nominal output voltage (AC)	230 V/400 V
Max. output current	14,5 A
Network frequency	50 Hz
Dimension (W/H/L)	470 mm/730 mm/240 mm
Weight	kg

2.2 Fronius Symo 12.5-3-M

Fronius Symo is a three-phase inverter without a transformer, with a nominal power of 12.5 kW and a maximum efficiency of 97,6 %, adapted to any system size.

Thanks to the possibilities provided by SuperFlex Design, Fronius Symo is optimal for curved roofs or roofs that are differently oriented. Standard internet connection via WLAN or Ethernet, as well as easy integration of the components from other manufacturers, make Fronius Symo one of the most adaptable inverters on the market in terms of communications. The module interface, moreover, allows a dynamic power management and a clear view of the local consumption. Furthermore, the inverter is equipped with protective devices that include DC insulation, DC disconnector, overload protection by shifting operating point or power limitation, and pole reversal protection [11].

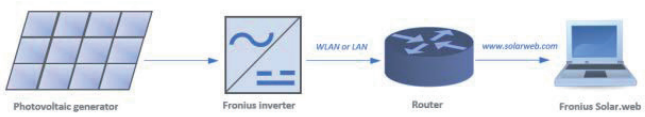

Figure 2. Connection of Fronius Symo inverter with PV and communication system [11]

The technical parameters and specification of Fronius Symo 12.5-3-M are shown in Table 2.

Table 2 Technical parameters of Fronius Symo 12.5-3-M inverter [11]

Parameter	Value
Max. input (DC) power	18.800 Wp
Max. input (DC) power	1.000 V
Input voltage operating range	370 – 800 V
Max. output (AC) power	12.500 W
Num. of MPPT units	2
Nominal output voltage (AC)	230 V/400 V
Max. output current	18 A
Network frequency	50 Hz
Dimension (W/H/L)	510 mm/725 mm/225 mm
Weight	34,8 kg

3. MODBUS TCP/IP

Modbus is an application layer messaging protocol, positioned at the seventh level of the Open Systems Interconnection (OSI) model, which enables Client/Server communication between devices connected to different buses or networks. Modbus is standard, open-source and the most commonly used network protocol in an industrial production environment [13]. It is a request and response protocol, implemented by Master/Slave or Client/Server relationship. In a Master/Slave relationship, the communication happens in the pair – one device must initiate the request and then wait for the response. The master is responsible for initiating each interaction. The Human Machine Interface (HMI) or SCADA system is commonly master, while the slave is commonly Programmable Logic Controller (PLC) or sensor. The contents of these requests and responses, and the network layers through which they are sent, are defined by different protocol layers. The Modbus message consists of a protocol data unit (PDU) which is independent of communication layers [34]. Modbus PDU format is defined like the function code followed by the associated data set. The PDU specification defines the basic concepts for data access and manipulation.

Data collected via Modbus are stored in address ranges or in one of four memory blocks: coils, discrete inputs, holding registers and input registers. Depending on the industry specifications or application, names of blocks may vary. With the specified memory blocks, data types and master-lave access rights are also defined. Slave devices have a direct access to data that is locally saved on the devices. In contrast, the master must require access to this data via various function codes. In addition to the Modbus protocol functionality defined in the PDU, multiple network protocols can be used. The most common protocols are serial and TCP / IP (Transmission Control Protocol / Internet Protocol), but others such as UDP (Unit Data Protocol) can be used. To transfer data across layers, Modbus includes an ADU (Application Data Unit) which is adapted to each network protocol. Modbus requires certain data to provide reliable communication. Unit ID or addresses are used in each ADU format to provide application layer routing information. Each ADU comes with a full PDU, which includes function code and associated data for the default request. For reliability, each me-

Marija Čuljak, Mateo Beus, Hrvoje Pandzic, Development of a LabVIEW - Based Data Logging and Monitoring Application for a Photovoltaic Power Plant at FER, Journal of Energy, vol. 70 Number 3 (2021), p. 14–18
https://doi.org/10.37798/2021703133

ssage includes the information error checking. Finally, all ADUs allow determining the beginning and end of the request frame. The three standard ADU formats are: TCP, RTU, and ASCII. RTU and ASCII are ADUs that are used over a serial line, while TCP is used over TCP/IP or UDP/IP networks. TCP/IP determines the rules of data exchange via the Internet by providing end-to-end communication that identifies the rules, e.g. how to divide data into packets, and how to address, transmit, direct or receive data at the destination. The protocol is designed to make networks dependable, with the ability to automatically recover from a failure of any device on networks. TCP defines how applications can create communication channels in a network. It also manages the way a message is compiled into smaller packets before being transmitted over the Internet and reassembled in the correct order at the destination address. IP defines how to address and route each packet to the right destination. Each computer connected to the network checks the IP address to determine where to forward the message. Considering adaptable and ubiquitous physical network (Ethernet) with universal network standard (TCP/IP) and independent presentation data by the manufacturer, Modbus provides an open and available data exchange network. It is easy to implement for any device that supports TCP/IP ports. The Modbus TCP ADU consists of a 7-byte header (MBAP) and N-byte data units (PDUs). The MBAP header includes Unit ID used to communicate via devices such as routers and gateways using a single IP address to support multiple and independent Modbus endpoints. The MBAP is also contained of a ProtocolID, which is commonly equal to zero, TransactionID used in the networks where more requests send at the same time, and Length. The inverters, Sunny Tripower 10000TL and Fronius Symo 12,5-3-M, have integrated Modbus TCP servers and they are supported for communication using the MODBUS TCP / IP communication protocol.

4. DEVELOPED APPLICATION FOR DATA LOGGING AND MONITORING

In this paper, the main aim is to collect measurements of relevant process quantities from the PV inverters such as current active power, total electricity produced, panel temperature, irradiation, ambient temperature, etc. The mentioned measurements are needed to save them to csv files in order to be available for further analysis and forecasting. Therefore, a communication between the PV inverters and the central computer needs to be established. The PV power plant consists of seven inverters and one data manager, which is used to collect temperature and irradiation data. Furthermore, it is necessary to design a graphical user interface (GUI), where the collected measurements from the PV power plant will be displayed. The graphical interface should consist of a main screen, on which it will be possible to select measurements from an individual inverter or total measurements for the entire PV power plant.

The State Machine structure used to develop the application in LabVIEW consists of three mains while loops: the loop to read data from the inverters, the loop to process and store data in a file and the loop to display data in the User Interface. The design pattern on which the application is based is Producer/Consumer. The Producer/Consumer design pattern is purposed at enhancing the data sharing between multiple loops running at different rates. It is used to separate the State Machine loops. one loop “produces” data, while the other loops “consume” them at different rates. The Producer/Consumer pattern is the most suitable for an application which acquires data while processing them in the order in which they are received. Consequently, collecting this data is much faster than their processing. If the producer and the consumers were in the same loop, the speed of collection data would be slowed down to match the data processing speed. That is why it is useful to separate the code into a data collection part and a data processing part.

Communication between the producer and consumer loops is done by using queues. The queues in the Producer/Consumer form are based on the FIFO (First In First Out) theory. In the Producer/Consumer form, queues can be applied using LabVIEW synchronization functions. The following advantages are derived using queues in the Producer/Consumer form:

- both loops are synchronized -- the consumer loop is executed only when the data is available in the queue;
- efficient code is created using queues;
- eliminating the possibility of losing data in the queue while adding new data.

The producer loop is commonly simpler than the consumer loop. The task of the producer loop is to read and collect measurements from the PV inverters, check the time and to forward the collected measurements to the consumer loop. The purpose of the consumer loop is to create folders in which the data will be stored in a csv file and use data for monitoring. Therefore, the program creates a new file every day in which the measurements for that day are saved. Also, for each new month or year, a new map will be created for better data visibility.

The queue should be initialized outside the producer loop using the “Obtain Queue” function and associate it with an appropriate data type. To add data to the queue within the producer loop, the “Enqueue Element” function is used. The consumer loop retrieves data from the queue created in the producer loop, and then removes the data from the queue using the “Dequeue Element” function. The first data inserted in the queue is also the first data to be removed from the queue. Moreover, before executing the program, the inverter initialization must be done. The required initialization data contains 3 elements: “Inverter Name”, “IP address” and “UnitID”. “Inverter Name” is the name of the inverter, “IP address” is the address over which measurements are sent from an individual inverter and “UnitID” is the identification number of each inverter. “UnitID” for SMA inverters can be freely configured within the range of 3 to 123, and the default value is 3. With Fronius Symo inverters, “UnitID” is equal to the number of inverter, and it can be configured using the control panel on the inverter.

4.1 User Interface

The front panel of this application is in fact a graphical user interface that is characterized by simplicity and clarity. The interface displays measurements that give users an insight into the current situation, but also the possibility of their further processing and analysis. The interface consists of nine tabs:

- Data Manager
- Sunny Tripower 1
- Sunny Tripower 2
- Sunny Tripower 3
- Fronius Symo1
- Fronius Symo 2
- Fronius Symo 3
- Froius Symo 4
- Data list

In Figure 3, the initial “Data Manager” tab shows data read from the device of the same name, radiation, temperature of PV modules and ambient temperature. Also, the total measured active power for the PV power plant in the period of the last hour is shown. At the top of the interface, there is an indicator that turns red if a communication error occurs.

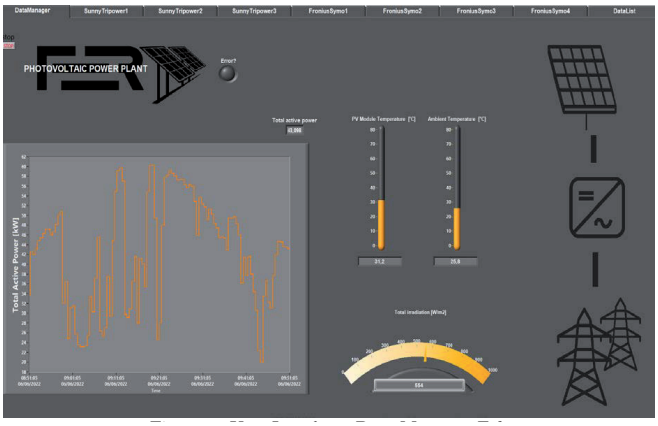

Figure 3. User Interface - Data Manager Tab

On the next seven tabs with inverter names, the interface is the same, except the measurements are adjusted for the corresponding inverter. The tabs are intended for instant display of all measured quantities. Displaying the measured quantities in real-time is a great advantage because the current state of the system can be obtained. Also, the current display gives an insight into whether the device is working properly. The measured quantities are displayed in two ways: numerically and graphically, as shown in Figure 4 for Fronius Symo 1 inverter. Possible causes of data deviations may be inverter malfunction, communication error or short-term atmospheric disturbances that may affect the sudden change of physical quantities. All measured quantities are read from inverters installed in SmartGrid Laboratory at UNIZG-FER [14].

Marija Čuljak, Mateo Beus, Hrvoje Pandzic, Development of a LabVIEW - Based Data Logging and Monitoring Application for a Photovoltaic Power Plant at FER, Journal of Energy, vol. 70 Number 3 (2021), p. 14–18
https://doi.org/10.37798/2021703133

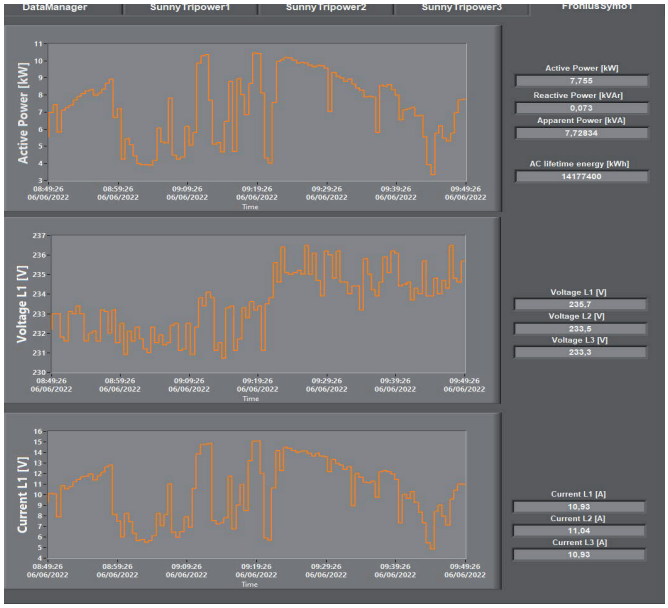

Figure 4. User Interface - Fronius Symo 1

The last tab “Data List” shows a list of the last 200 collected measurements. In this way, a better visibility of historical data to the user is ensured. At the bottom of this tab, there is also a file path through which the user accesses the csv file where can find all collected measurements of the current day.

4.2 Display of collected measurements

The graphs show the measurements of the active power of the inverters [kW], the radiation [W/m²] and the temperature of the PV modules [°C] and the ambient temperature [°C] for June 6th, 2022 (Figures 5-8). An increase in the temperature of solar cells is always accompanied by an increase in the intensity of the solar cells radiation and the output power of the photovoltaic module depends linearly on the temperature of the PV modules [15].

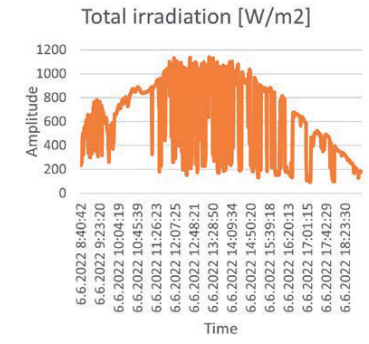

(a)

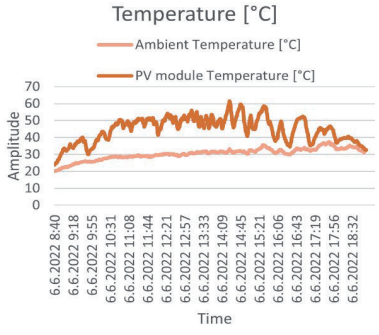

(b)

Figure 5. Graphical representation of measurements on June 6th, 2022: (a) Total irradiation [W/m²]; (b) PV module and ambient temperature [°C]

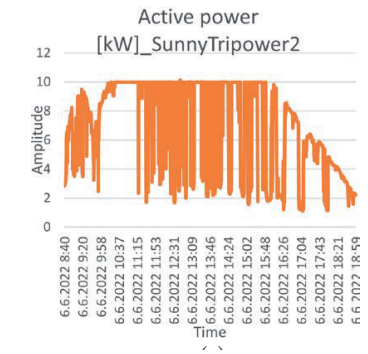

(a)

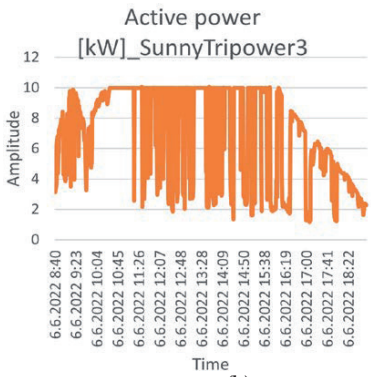

(b)

Figure 6. Graphical representation of measurements on June 6th, 2022: (a) Active Power of Sunny Tripower 2 [kW]; (b) Active Power of Sunny Tripower 3 [kW]

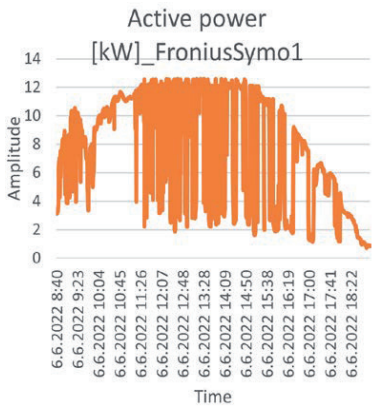

(a)

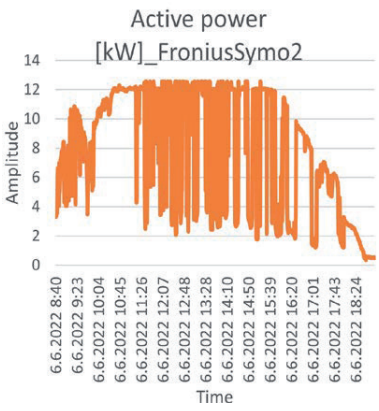

(b)

Figure 7. Graphical representation of measurements on June 6th, 2022: (a) Active Power of Fronius Symo 1 [kW]; (b) Active Power of Fronius Symo 2 [kW]

Marija Čuljak, Mateo Beus, Hrvoje Pandzic, Development of a LabVIEW - Based Data Logging and Monitoring Application for a Photovoltaic Power Plant at FER, Journal of Energy, vol. 70 Number 3 (2021), p. 14–18
https://doi.org/10.37798/2021703133

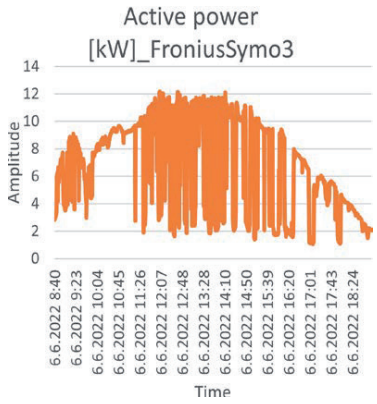

(a)

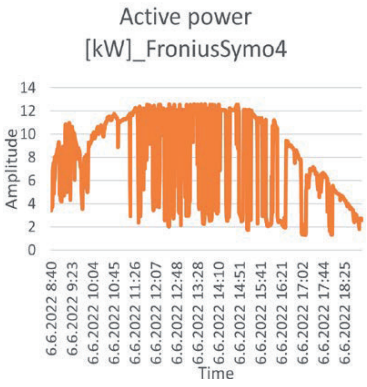

(b)

Figure 8. Graphical representation of measurements on June 6th, 2022: (a) Active Power of Fronius Symo 3 [kW]; (b) Active Power of Fronius Symo 4 [kW]

CONCLUSION

In this paper, an application is presented for logging and visualization of measurements from a PV power plant located at the University of Zagreb Faculty of Electrical Engineering and Computing. The main aim of this paper is to increase the visibility of the PV power plant by implementing a system for monitoring and collecting measurements in a real-time. The technical characteristics of PV inverters Sunny Tripower 10000TL-20 and Fronius Symo 12,5-3-M are described in detail. The communication between the inverters and the central computer is achieved by the Modbus TCP/IP protocol that enables an open and accessible network for the exchange of process data in a simple and reliable way. The graphical language LabVIEW is used to create the application that allows analysis, processing and display of data in an intuitive way. LabVIEW uses the Producer/Consumer format to improve program performance to a certain level and enable easy multi-process operations performed at different speeds. The collected measurements are displayed on the developed User Interface which shows the current condition. The created csv files contain accurate 15-minute measurements and provide detailed insight into the operation of the PV power plant.

Therefore, this application achieved efficient and synchronized measurements, collecting and processing data in one place, as well as real-time communication, whereby the reliability of the electric power system is increased. This system with minor upgrades can be easily used to collect data and monitor large PV modules and systems or for industrial purposes.

REFERENCES

[1] B. Andò, S. Baglio, A. Pistorio, G. M. Tina and C. Ventura, "Sentinella: Smart Monitoring of Photovoltaic Systems at Panel Level," in *IEEE Transactions on Instrumentation and Measurement*, vol. 64, no. 8, pp. 2188-2199, August, 2015.

[2] N. Čović, F. Braeuer, R. McKenna, and H. Pandžić, "Optimal PV and Battery Investment of Market-Participating Industry Facilities," in *IEEE Transactions on Power Systems*, vol. 36, no. 4, pp. 3441-3452, July 2021.

[3] I. Allafi, T. Iqbal, "Low-cost SCADA system using arduino and reliance SCADA for a stand-alone photovoltaic system," in *Journal of Solar Energy*, pp.1-8, January, 2018.

[4] H. Pandžić, D. Bošnjak, I. Kuzle, M. Bošković, and D. Ilić, "The Implementation of Smart Metering Systems for Electricity Consumption in Croatia," in *Proceedings of 17th Symposium IMEKO TC 4 / 3rd Symposium IMEKO TC 19 – Session 12,* Kosice, Slovakia, September 8-10, 2010.

[5] M. Zahran, Y. Atia A. Al-Hussain, I. El-Sayed, "LabVIEW based monitoring system applied for PV power station" in *Proceedings of the 12th WSEAS International Conference on Automatic Control, Modelling and Simulation (ACMOS'10),* Catania, Italy, May, 2010 , pp. 65-70.

[6] S. Vergura and E. Natangelo, "Labview interface for data analysis of PV," *2009 International Conference on Clean Electrical Power*, 2009, pp. 236-241.

[7] A. Chouder A, S. Silvestre, B. Taghezouit, E. Karatepe, "Monitoring, modelling and simulation of PV systems using LabVIEW" in *Solar Energy,* vol. 91, no. 1, pp. 337-349, May, 2013.

[8] D. Šljivac, B. Nakomčić-Smaragdakis, M. Vukobratović, D. Topić, Z. Čepić, "Cost-benefit comparison of on-grid photovoltaic systems in Pannonian parts of Croatia and Serbia" in *Tehnički vjesnik*, vol. 21, no. 5, pp. 1149-1157, October, 2014.

[9] C.G. Popovici, S.V. Hudişteanu, T.D. Mateescu, N.C. Chereches, "Efficiency improvement of photovoltaic panels by using air cooled heat sinks" in *Energy Procedia,* vol. 85, pp. 425-432, January, 2016.

[10] "Sunny Tripower Smart Energy, " SMA Solar Technology AG, [Online]. Available: https://www.sma.de/en/products/hybrid-inverters/sunny-tripower-smart-energy.html. [Accessed 14 06 2022].

[11] "Fronius Symo – Maximum flexibility for the applications of tomorrow, " Fronius International GmbH, [Online]. Available: https://www.fronius.com/en-gb/uk/solar-energy/installers-partners/technical-data/all-products/inverters/fronius-symo/fronius-symo-12-5-3-m. [Accessed 14 06 2022].

[12] SMA, "PV Inverter "SUNNY TRIPOWER 8000tl / 10000tl / 12000tl / 15000tl / 17000tl" Installation Manual, 2012.

[13] Q. Bai, B. Jin, D. Wang, Y. Wang, X. Liu, "Compact Modbus TCP/IP protocol for data acquisition systems based on limited hardware resources" in *Journal of Instrumentation*, vol. 13., no. 4., April, 2018.

[14] "Smart Grid Laboratory (SGLab)," Faculty of Electrical Engineering and Computing, Department of Energy and Power Systems, University of Zagreb, Online]. Available: https://sglab.fer.hr/. [Accessed 16 06 2022].

[15] S. Dubey, J.N. Sarvaiya, B. Seshadri, "Temperature dependent photovoltaic (PV) efficiency and its effect on PV production in the world–a review" in *Energy Procedia*, vol. *33*, pp.311-321, January, 2013.

Journal of Energy

VOLUME 70 Number 3 | 2021

journal homepage: http://journalofenergy.com/

Josip Đaković [1]
HEP – Distribution System Operator
Slavonski Brod, Croatia
josip.dakovic@hep.hr

Bojan Franc
University of Zagreb
Faculty of electrical engineering and computing
Zagreb, Croatia
bojan.franc@fer.hr

Igor Kuzle
University of Zagreb
Faculty of electrical engineering and computing
Zagreb, Croatia
Igor.kuzle@fer.hr

Yongqian Liu
North China Electric Power University
New Energy School
Beijing, China
yqliu@ncepu.edu.cn

[1] Statements expressed in the paper are author's own opinions, they are not binding for the company/institution in which author is employed nor they necessarily coincide with the official company/institution's positions.

Deep Neural Network Configuration Sensitivity Analysis in Wind Power Forecasting

SUMMARY

The trend toward increasing integration of wind farms into the power system is a challenge for transmission and distribution system operators and electricity market operators. The variability of electricity generation from wind farms increases the requirements for flexibility needed for the reliable and stable operation of the power system. Operating a power system with a high share of renewables requires advanced generation and consumption forecasting methods to ensure the reliable and economical operation of the system. Installed wind power capacities require advanced techniques to monitor and control such data-rich power systems. The rapid development of advanced artificial neural networks and data processing capabilities offers numerous potential applications. The effectiveness of advanced deep recurrent neural networks with long-term memory is constantly being demonstrated for learning complex temporal sequence-to-sequence dependencies. This paper presents the application of deep learning methods to wind power production forecasting. The models are trained using historical wind farm generation measurements and NWP weather forecasts for the areas of Croatian wind farms. Furthermore, a comparison of the accuracy of the proposed models with currently used forecasting tools is presented.

KEY WORDS

Wind power forecasting, deep learning, recurrent neural networks, LSTM, big data analytics, wind farms

INTRODUCTION

Energy generation from renewable energy sources (RES), of which a high proportion is wind farm (WF) generation, will have an increasingly important impact in achieving low-carbon development of the electric power system (EPS). Although the integration of wind farms brings many benefits from an environmental point of view, the unpredictable and variable nature of WF generation poses many challenges for EPS operators (ensuring adequate ancillary services, economic dispatching of power plants, dynamic stability of the system), electricity market operators, and electricity producers and traders. One of the possible solutions to the above challenges is the development of advanced tools and methods for reliable short-term forecasting of wind farm generation [1,2]. Wind power forecasting is becoming increasingly important in grid planning, optimization, and control as more and more energy is generated from inherently intermittent renewable sources. For practical purposes, the forecast time horizon can be divided into short-term (up to 12 hours ahead) and long-term (up to 72 hours ahead) forecasts [3,4]. Short-term forecasts can be used to regulate the system and operate the intraday electricity market, while long-term forecasts are often used to plan power plant dispatch and the day-ahead electricity market [5]. In recent decades, the amount of available information and computer power have grown very rapidly, so forecasting methods have evolved from simple statistical and physical models to much more complex statistical models, including the concepts of machine learning and, more recently, deep learning [6]. The aforementioned methods of Big Data analysis deal with huge amounts of complex data that are not suitable for processing with conventional algorithms. Methods based on a special type of recurrent neural network (RNN) with long short-term memory (LSTM) have proven highly successful in modeling long-term dependencies of meteorological variables and energy generation [7,8,9]. This is because LSTM-based networks are designed to learn dependencies among sequences of data. Weather forecast (Numerical weather prediction-NWP), as the most important input for wind power forecasting, provides time-labeled sequences of forecast data suitable for training recurrent networks. However, the accuracy of the LSTM method depends significantly on the network configuration and pre-training parameterization, which is specific to each type of application.

Fig. 1 shows the classification of commonly used approaches and methods for wind power predictions. Therefore, the methods used in this paper can be classified as data-driven deep-learning methods for short-term point-forecast of a wind power plant production. In addition to the deterministic approach, research is also being conducted on the probabilistic quantification of prognostic results, which aims to reduce the uncertainty of the forecast using confidence intervals [10].

Josip Đaković, Bojan Franc, Igor Kuzle, Yongqian Liu, Deep Neural Network Configuration Sensitivity Analysis in Wind Power Forecasting, Journal of Energy, vol. 70 Number 3 (2021), p. 19–24
https://doi.org/10.37798/202170389

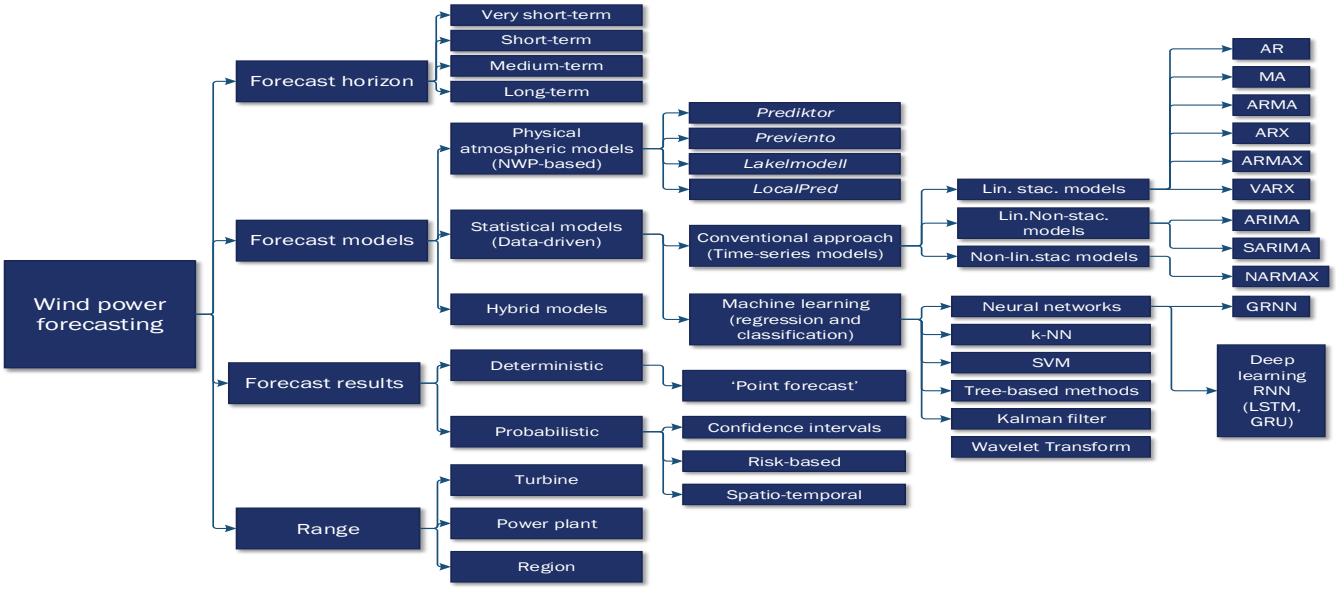

Figure 1: Wind power forecasting approaches [5]

RECURRENT NEURAL NETWORKS

The main feature of conventional neural networks, such as densely interconnected networks and convolutional networks, is that they have no internal memory. Each input is processed independently without determining or comparing conditions between inputs. To process a sequence or time series with these networks, it is necessary to represent the entire sequence at once: turn it into a single data point as the network input [11]. Such a neural network is called a *feedforward neural network* and is often used in load forecasting [12][13]. Unlike traditional neural networks (NN), recurrent neural networks process series (sequences) by iteratively traversing the elements of a sequence and retaining the states that contain information about the previous data. RNN is a type of neural network with an inner loop and memory. The internal state of the RNN is reset between the processing of two different independent sequences, so a sequence is still considered a data point: one input to the network. What changes is that the data point is no longer processed in one step; the iterates internally over the sequence elements. Simple (basic) recurrent networks face the problem of a vanishing gradient when training long sequences using deep networks (networks with multiple layers), which makes them practically useless. The solution to the above problem was proposed in 1997 (Hochreiter and Schmidhuber) in the form of networks with long-lasting short-term memory, but their practical application has been realised only in the last decade. Processing data in the LSTM layer is shown in Fig. 2 LSTM enables the data (hidden state of cell h_t) at any moment t of the input sequence (x_t) to be transferred into long-term memory (C_t) at a later moment in time and deleted from it, if necessary. Stated functions are realized with the help of special gate functions (f_t, i_t, o_t). In short, LSTM-based models learn relevant dependencies across the input sequence, avoiding the vanishing gradient problem during training.

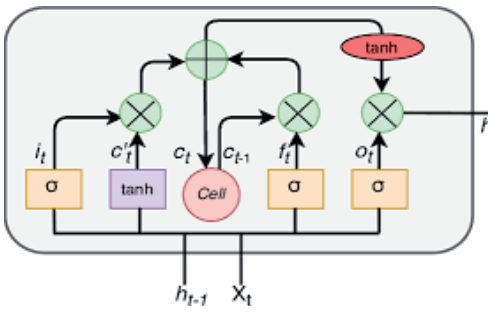

Figure 2: Data flow in LSTM cell in one step

2.1 Forecasting time sequences of wind farm generation

Sequence forecasting is different from other types of supervised machine learning in that it requires to maintain the temporal order of sequence values during model training and testing. Apart from numerical time sequences, sentences in text translation represent another type of commonly used sequential data for supervised machine learning. In the present case of wind power forecasting, time series of Croatian WFs power generation are converted into time sequences by segmenting continuous two-year time series into partially overlapping sequences.[1] For this reason, the paper deals with the time sequences of WF power output.

In general, forecasting problems with sequential data can be divided into four groups:

1. forecasting of the following value of the sequence;
2. sequence classification (forecast of the class according to the input sequence);
3. sequence generation (e.g., by generating text);
4. sequence-to-sequence prediction.

According to the form of available input data that can be used to forecast wind farm generation (sequential forecasts of atmospheric conditions from meteorological models) and obtaining historical power generation data from the SCADA system, a sequence-to-sequence problem can be formed: mapping sequences of (historical) weather forecasts (mostly wind speed and direction) to (historical) wind farm power generation sequences [14]. Fig. 3 shows the process of data preparation for training, validation, and testing of the models used in this work.

Input data, i.e., time series of historical measurements of realized production and historical NWP forecasts are 'cut' into 72-hour long sequences[2], aligned by timestamp, and merged in the form of 3D arrays (tensors) with dimensions: (sequence samples, horizon (72h), predictors). Mathematically speaking, the model of deep learning in this case is a composition of a matrix (tensor functions), which form is defined in advance using the so-called model layers. During the training process, the matrix weights of the predefined structure of the model are adjusted, to achieve an optimal mapping model from input predictors to output WPP production.

During the training and validation process, the available predictors (in this case wind speed and direction) are mapped to the actual power output of

1 The power generation sequences should be aligned according to time steps with overlapping weather forecasts, which in the observed case are generated every 6 hours for the following 72 hours, which means that there are several forecasts for the same moment.

2 In this paper, the sequence is considered as a 72-h long part of the time series of the realized power measurement or NWP forecast.

Josip Đaković, Bojan Franc, Igor Kuzle, Yongqian Liu, Deep Neural Network Configuration Sensitivity Analysis in Wind Power Forecasting, Journal of Energy, vol. 70 Number 3 (2021), p. 19–24
https://doi.org/10.37798/202170389

the WFs under consideration. The difference between training and validation is that validation is used only to monitor the accuracy of the model during the training process. After the model has been trained, new predictors data is inserted into the model for the testing process for which training has not yet been performed, so that the model produces a forecast based on a "learned" relationship between the weather forecasts and the corresponding power output of the wind farm.

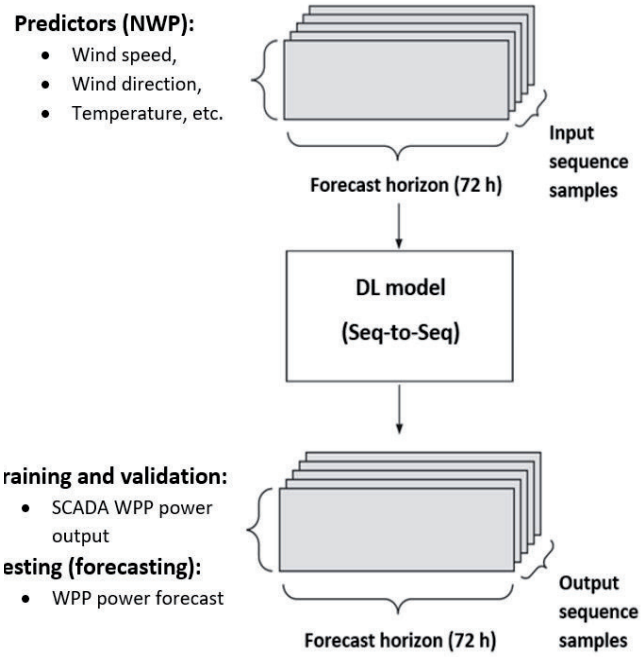

Figure 3: Modeling sequential forecasting model

2.2 Deep learning model for sequential data

The basic structural unit in a deep neural network is a layer. The layer is a module for data processing, which takes one or more tensors (data arrays) as input and returns one or more tensors as output. Some layers have no internal states (dense layers), but RNN-based models have layers with internal states and multiple weight matrices that contain the network's 'intelligence'. Sequential data is usually formed as 3D tensors with the following dimensions: (samples, time steps/horizon, predictors/feature) processed by recurrent layers such as LSTM and GRU (Gated Recurrent Unit). A deep learning model is built by "assembling" compatible layers in an appropriate configuration depending on the nature of the problem and the form of the input data. The layers of the model are usually arranged sequentially, meaning that the output of one layer represents the input to the next layer, but other topologies are also possible. In addition to the choice of network architecture, it is necessary to choose a loss function that is minimized during training and represents the accuracy measure between actual values and predictions. The value of a loss function, i.e., the error, is propagated through back-connections in layer weigh matrices (backpropagation through time) by using an optimization algorithm (e.g., Adam) based on stochastic gradient descent. For network training, the Adam optimizer was used because it is considered a very effective and fast training algorithm for deep neural networks. The learning is usually completed when the gradient values of all weight parameters are equal or close to zero. The process of model training is shown in Fig. 4. The choice of the appropriate loss function depends on the nature of the problem (regression, classification), and mean square error is most commonly used for the aforementioned type of sequential numerical data. Training a deep learning model requires considerable computational resources, which determine both the possible 'depth' of a model and the speed of training, which is usually performed by advanced graphics processing units [17].

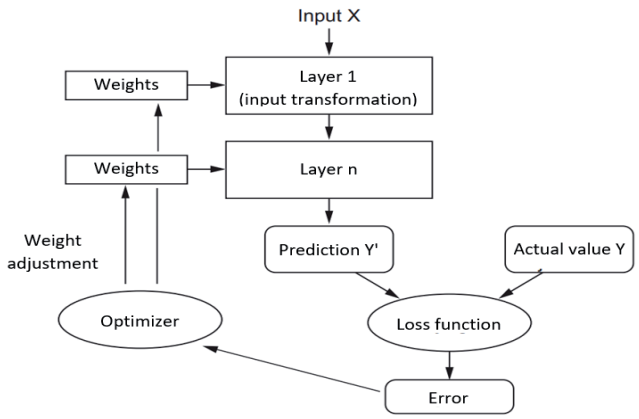

Figure 4: Process of training deep learning model

3. APPLICATION OF DEEP LEARNING TO FORECASTING WF GENERATION

Before the actual Deep Learning model is created, the input data must be prepared, which is usually not in a format suitable for model training. Preparation requires data clearing (e.g., removing unreal values, filling voids, etc.), data timestep alignment (e.g., reducing it to hourly values), and forming appropriate data tensors. In the following section, the process of model training and testing on real two-year data of a wind farm in Croatia is presented.

3.1 Wind farm data

Fig. 5 presents the two-year power generation data (from January 2018 to January 2020) of the considered WF in terms of measured wind speed and direction, i.e., the real wind power dependence curve of the considered WF. The wind rose (wind distribution by directional frequency) is shown in Fig. 6 with average wind speeds on the radial axis (e.g., in the interval from northwest to west wind (135°- 180°) the average wind speed is 7.72 m/s). Moreover, the average wind speed is proportional to the frequency of the wind direction, the predominant winds being bora and mistral. Fig. 7 shows the distribution of wind speed at the site with the marking of the average wind speed of 6 m/s (red line). Finally, Fig. 8 shows the correlation matrix of the measurement parameters in the SCADA system (wind speed and direction, operating power, temperature, and pressure).

It can be observed that wind speed has the highest correlation with power production (more than 0.8), while other meteorological parameters such as air direction, temperature, and pressure have a significantly lower correlation with power. The explanation for the low correlation between wind direction and production can be found in the problem of hourly averaging of wind direction (e.g., a wind whose direction oscillates between 0 and 360 degrees can lead to a mean value that suggests the opposite direction) and the possibility of modern WTG to rotate turbine nacelles in the optimal wind direction.

It is expected that wind speed has a positive correlation with the performance of WF power higher than 0.9, while wind direction, pressure, and temperature have a slightly negative correlation with the performance of the wind farm's power.

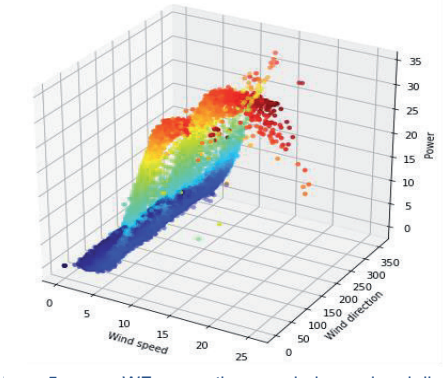

Figure 5: WF generation vs. wind speed and direction

Josip Đaković, Bojan Franc, Igor Kuzle, Yongqian Liu, Deep Neural Network Configuration Sensitivity Analysis in Wind Power Forecasting, Journal of Energy, vol. 70 Number 3 (2021), p. 19–24
https://doi.org/10.37798/202170389

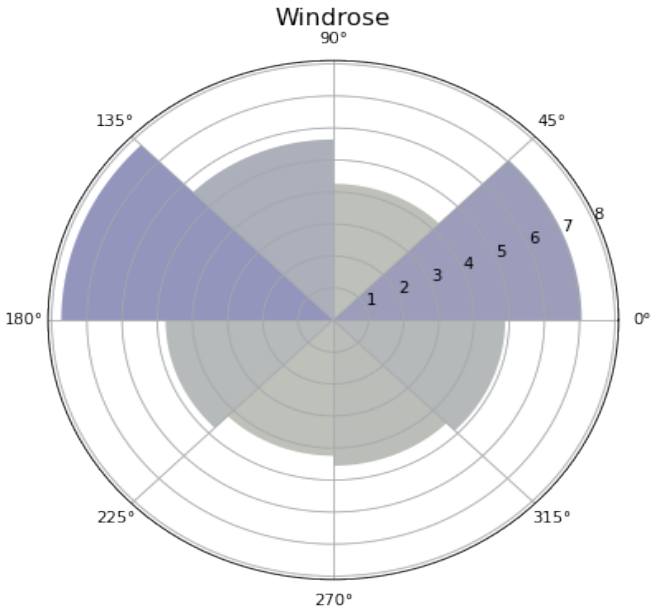

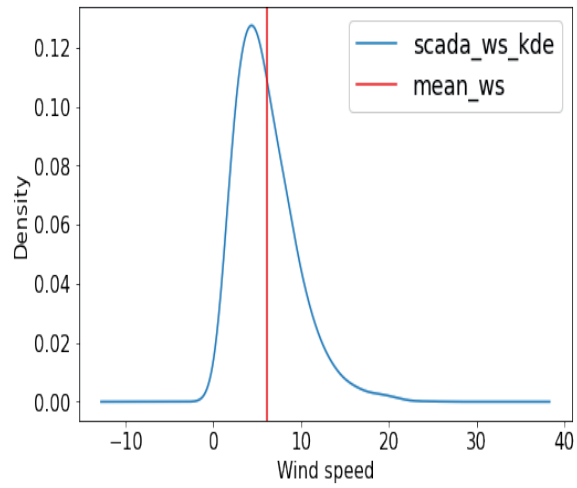

Figure 6: Wind rose with mean wind speed

Figure 7: Distribution of WS on WF's location

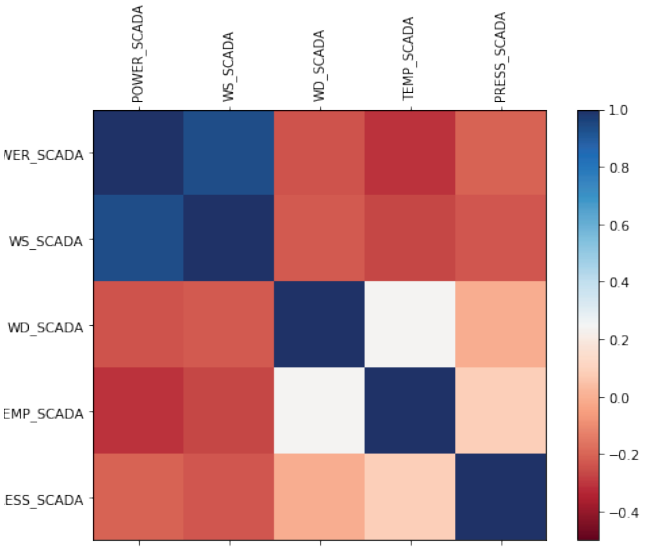

Figure 8: SCADA correlation matrix

3.2 Model

The input predictors of the model were two-year forecasts of wind speed and direction from the Aladin 2 meteorological model (NWP). The wind speed and direction forecasts are available in the form of 72-hour-long hourly sequences computed four times a day, i.e., every six hours. The total number of available sequences in a two-year period is regularly divided into three parts: training, validation, and test in the ratio of 70%, 10%, and 20% (the ratio is randomly selected). The Python 3 programming language was used to build the model, with the specific modules for deep learning, Keras, and TensorFlow for operations with tensors. Fig. 9 shows the structure of the two models used. The first model (Fig. 9a) consists of one LSTM layer and one dense layer. The mentioned model processes sequences only in a chronological way. The other model used is shown in Fig. 9b) (bidirectional LSTM), which processes sequences in a chronological and reverse manner. The internal states of the LSTM cell of forward and reverse sequences are combined with one of the possible functions (summation, multiplication, concatenation, etc.) and forwarded to the next layer (Fig. 9c).

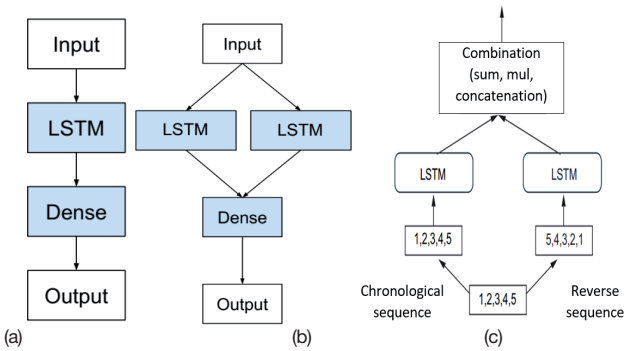

Figure 9: a) one-directional LSTM model (model 1); b) bidirectional LSTM model (Bi-LSTM) (model 2); c) Working principle of BI-LSTM

Fig. 10 presents layers and belonging parameters (report from Tensorflow environment) that are adjusted during training. The bidirectional LSTM model has almost twice as big internal memory. The size of the internal memory is a random (hyper) parameter of the model, like many other parameters that should be set before training.

```
Model: "sequential_15"
_________________________________________________________________
Layer (type)                 Output Shape              Param #
=================================================================
lstm_15 (LSTM)               (None, 72, 50)            10600
_________________________________________________________________
dense_26 (Dense)             (None, 72, 50)            2550
_________________________________________________________________
dense_27 (Dense)             (None, 72, 1)             51
=================================================================
Total params: 13,201
Trainable params: 13,201
Non-trainable params: 0


Model: "sequential_10"
_________________________________________________________________
Layer (type)                 Output Shape              Param #
=================================================================
bidirectional_9 (Bidirection multiple                  21200
_________________________________________________________________
dense_16 (Dense)             multiple                  2550
_________________________________________________________________
dense_17 (Dense)             multiple                  51
=================================================================
Total params: 23,801
Trainable params: 23,801
Non-trainable params: 0
```

Fiure 10: a) Model 1 parameters; b) Model 2 parameters

Josip Đaković, Bojan Franc, Igor Kuzle, Yongqian Liu, Deep Neural Network Configuration Sensitivity Analysis in Wind Power Forecasting, Journal of Energy, vol. 70 Number 3 (2021), p. 19–24
https://doi.org/10.37798/202170389

4. RESULTS

Fig. 11 shows the process of training and validating models 1 and 2. The training of the model is terminated when the loss function has not changed over a certain number of epochs (e.g., 10 epochs) in the validation data. Fig. 11b) shows the root mean square error (RMSE) between the forecasted sequences and the real values on the validation data (the root of the loss function on the validation data), i.e., the validation metrics of the model. It is obvious that model 2 reaches the minimum of the loss function faster, so the overall RMSE is more favorable in the case of bidirectional LSTM, which is due to the larger internal memory of model 2.

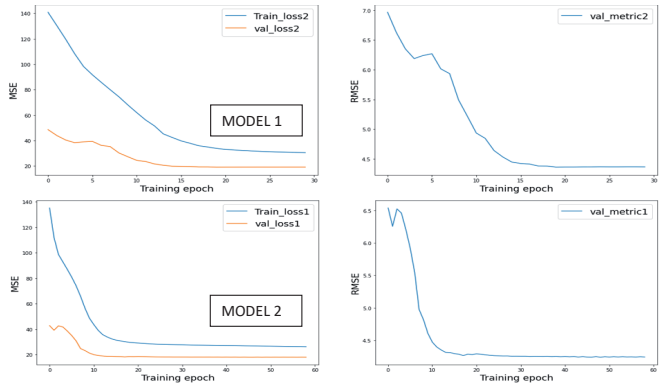

a) b)

Figure 11: a) Loss function of models 1 and 2 (training and validation) b) metrics of model's accuracy on validation data (RMSE)

Fig. 12 presents the comparison of commercial tools (WPPT2 and WPPT3) with two test data samples, in comparison with real measurements of the SCADA system and comparison with forecasts of the presented deep learning models. In addition, it is possible to combine the forecasts of both models to obtain an average prediction that can provide better results (red curve - ensemble_pred). It can be seen that the proposed models provide forecasts of commercial accuracy with a relatively shallow model structure. Of course, more complex, and 'deeper' models could provide better results. It is interesting to note that the WPPT2 tool uses the same NWP forecasts (Aladin 2) as the input data used in this work, while WPPT3 uses multiple NWP forecast sources (Enfor). Fig 12 c) presents a horizon RMSE performance comparison on the test dataset (500 sequences) where it can be seen that the WPPT2 model had the worst while the ensembled model had the highest accuracy.

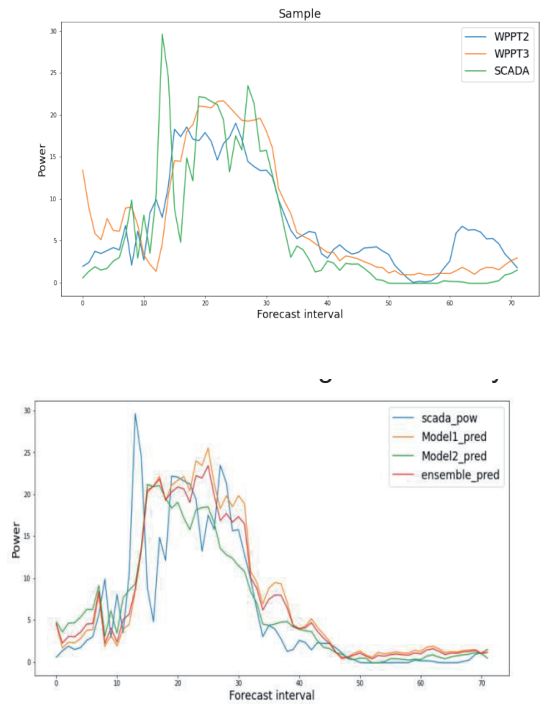

a)

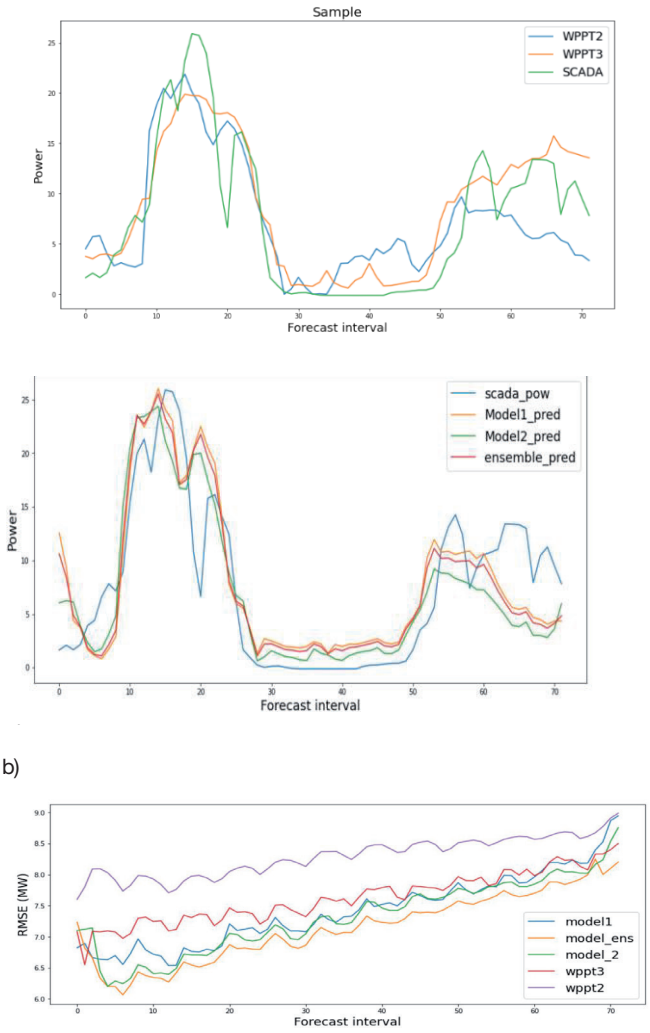

b)

c)

Figure 12: Model comparison with commercial tools and SCADA measurements; a) sample 1; b) sample 2; c) Horizon RMSE comparison (test dataset)

CONCLUSION

This paper shows one of the approaches to applying deep learning to wind power forecasting using recurrent networks for sequential data. The process of data preparation and the data structure, as well as the model structure, are explained. Finally, a comparison of the forecasts obtained by the proposed methodology and commercial tools is presented using two samples, which provides insight into the accuracy of the forecasts obtained with methods of deep learning. The results showed that deep recurrent LSTM-based networks can outperform commercially available forecasting tools when trained using only the wind speed forecast as an input feature. Future research will focus on developing more complex models of deep learning to increase overall accuracy.

Josip Đaković, Bojan Franc, Igor Kuzle, Yongqian Liu, Deep Neural Network Configuration Sensitivity Analysis in Wind Power Forecasting, Journal of Energy, vol. 70 Number 3 (2021), p. 19–24
https://doi.org/10.37798/202170389

REFERENCES

[1] A. M. Foley, P. G. Leahy, A. Marvuglia and E. J. McKeogh, *Current methods and advances in forecasting of wind power generation*, Renewable Energy, vol. 37, pp. 1-8, January 2012 https://www.sciencedirect.com/science/article/pii/S0960148111002850

[2] J. Jung and R. Broadwater, *Current status and future advances for wind speed and power forecasting*, Renewable and Sustainable Energy Reviews, vol. 31, pp. 762-777, March 2014 https://www.sciencedirect.com/science/article/pii/S1364032114000094

[3] G. Giebel, *The state-of-the-art in short-term prediction of wind power - A literature overview*, Project ANEMOS, August 2003 https://www.osti.gov/etdeweb/servlets/purl/20675341

[4 Y. Ding, *Data science for wind energy*, Chapman and Hall/CRC, p. 424, December 2020

[5] J. Đaković and I. Kuzle, *Status and classification of methods for forecasting electricity generation from wind farms*, 13th Symposium on power system management HRO Cigre, Rovinj, Croatia, November 2018 https://www.bib.irb.hr/971989

[6] I. Kuzle, M. Klarić and H. Pandžić, *Feasibility assessment of a wind power plant with insufficient local wind data using cascade-correlating neural network*, Strojarstvo, vol. 53, no. 6, pp. 455-462, December 2011 https://hrcak.srce.hr/file/126033

[7] V. Bali and A. Kumar, *Deep learning based wind speed forecasting-A review*, 9th International Conference on Cloud Computing, Data Science & Engineering, Noida, India, January 2019, https://ieeexplore.ieee.org/document/8776923

[8] L. Han, R. Zhang, X. Wang, A. Bao and H. Jing, *Multi-step wind power forecast based on VMD-LSTM*, IET Renewable Power Generation, vol. 13, no. 10, pp. 1690-1700, July 2019, https://ietresearch.onlinelibrary.wiley.com/doi/10.1049/iet-rpg.2018.5781

[9] J.-F. Toubeau, J. Bottieau, F. Vallée and Z. D. Grève, *Improved day-ahead predictions of load and renewable generation by optimally exploiting multi-scale dependencies*, IEEE Innovative Smart Grid Technologies - Asia (ISGT-Asia), December 2017 https://ieeexplore.ieee.org/document/8378396

[10] H. Zhang, Y. Liu, J. Yan, S. Han, L. Li and Q. Long, *Improved deep mixture density network for regional wind power probabilistic forecasting*, IEEE Transactions on Power Systems, vol. 35, no. 4, pp. 2549-2560, July 2020, https://ieeexplore.ieee.org/document/8982039

[11] F. Chollet, *Deep learning with Python*, Manning, p. 384, November 2017 https://www.manning.com/books/deep-learning-with-python

[12] I. Sičaja, A. Previšić, M. Zečević and D. Budiša, *Evaluation of load forecast model performance in Croatian DSO*, Journal of Energy, vol. 67, no. 2, pp. 54-62, June 2018 http://www.journalofenergy.com/index.php/joe/article/view/80

[13] N. Holjevac, C. Soares, I. Kuzle, *Short-term power system hourly load forecasting using artificial neural networks*, Journal of Energy, vol. 66, no. 1-4, pp. 241-254, December 2017 http://www.journalofenergy.com/index.php/joe/article/view/107

[14] K. Jurković, H. Pandžić and I. Kuzle, *Review on unit commitment under uncertainty approaches*, 38th International Convention on Information and Communication Technology, Electronics and Microelectronics (MIPRO 2015), Opatija, Croatia, May 2015 https://ieeexplore.ieee.org/abstract/document/7160438

[15] D.P. Kingma and J. Ba, *Adam: A method for stochastic optimization*, ICLR, p. 1-15, January 2017 https://arxiv.org/abs/1412.6980

[16] V. Bushaev, *Adam — latest trends in deep learning optimization*, October 2018, https://towardsdatascience.com/adam-latest-trends-in-deep-learning-optimization-6be9a291375c

[17] J. Brownlee, *Long short-term memory networks with Python*, ebook, p. 229, July 2018 https://machinelearningmastery.com/lstms-with-python/

Journal of Energy

VOLUME 70 Number 3 | 2021

journal homepage: http://journalofenergy.com/

Marija Šiško Kuliš
HEP Proizvodnja d.o.o
marija.sisko-kulis@hep.hr

Nikola Mijalić
HEP Proizvodnja d.o.o
nikola.mijalic@hep.hr

Senad Hodžić
University of Zagreb
JU „I srednja škola“ Cazin
senad-hodzic@live.com

Cavitation Detection on Hydraulic Machines

SUMMARY

This paper gives an engineering review of the phenomenon of cavitation on hydraulic machines: turbines, pumps and ships propellers. The types of cavitation and its consequences are presented by the cabinet study of the results of relevant researches on models and real plants. In the special focus of this paper are the techniques of exploration of cavitation erosion: visual examination, measurements of pressures and vibrations and CFD methods.

KEY WORDS

Cavitation, turbine, detection, pressure

1. INTRODUCTION

Liquids usually have characteristic that change chemical phase from liquid phase to vapour phase. Phase changes are introduction in cavitation phenomenon. Cavitation in cosmetic surgery is very positive phenomenon while for hydraulic turbomachinery is negative phenomenon. This is generally an undesirable phenomenon, which cannot be avoided, but scientists, engineers and businessmen can reduce its harmful effects by using various techniques, more or less successfully, by detecting cavitation. It is in focus of interest of this paper.
Cavitation as unwanted process appears at turbomachinery, and especially at water turbines pumps etc. Typical cavitation on hydraulic machines like water turbines and screw propeller are shown at Fig 1: a) Francis turbine – cavitation vortex [1], b) Ship propeller [2], c) Francis turbine - inlet cavitation [3], d) Francis turbine - outlet cavitation [3], f) pump cavitation, [4].

b) [2]

a) [1]

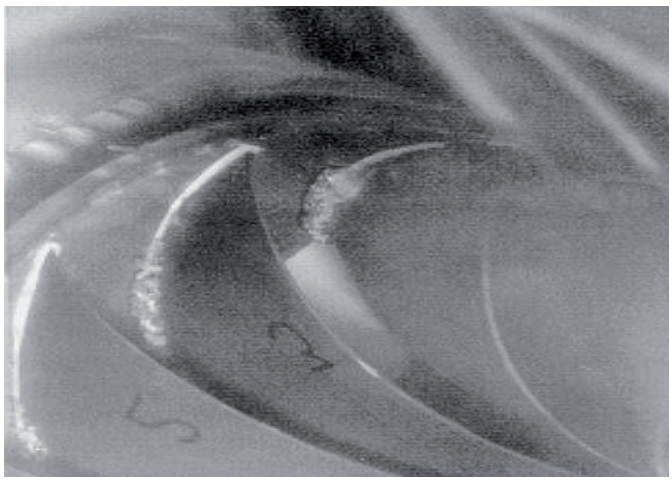

1 c) [3]

Marija Šiško Kuliš, Nikola Mijalić, Senad Hodžić, Cavitation Detection on Hydraulic Machines, Journal of Energy, vol. 70 Number 3 (2021), p. 25-32
https://doi.org/10.37798/202170328

d) [3]

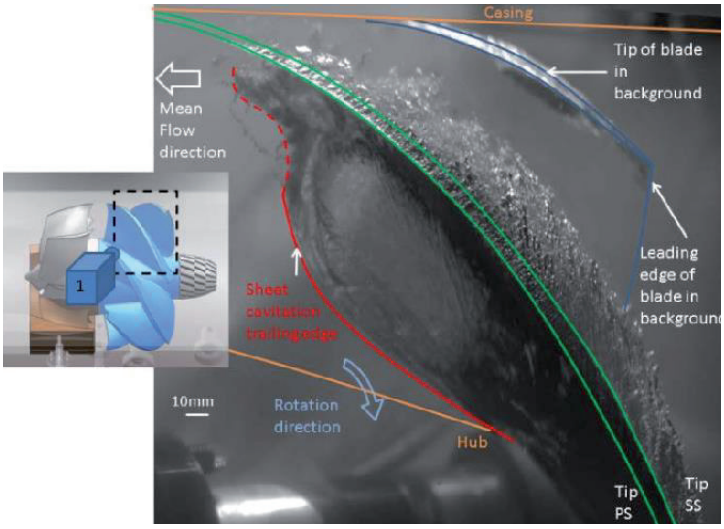

f) [4]

Figure 1. Cavitation on hydraulic machines

The occurrence of cavitation depends directly on the hydraulic performance of the machine, the rotor profile and material selection, and the mode of operation of the machine, percentage of dissolved gases, high temperatures and low viscosity, impurities in the form of particles and gas also have an effect on cavitation. [5] Also the geodetic height of machine is also very important.
Cavitation (Ger. *kavitazion*, franc. *cavitation*, lat. *cavitas*, *cavus*: hollow, cored) is cavity, empty space, [6].
Well, let's start with, every engineering methodology is always based on a clear and unambiguous analysis of the occurrence, process, or generally speaking, of an observed problem. Cavitation can be observed in two different ways as vaporous cavitation and as gaseous cavitation. For hydraulic machines vaporous cavitation is more frequent than the gaseous cavitation.
What is cavitation? In hydrodynamics cavitation is a phenomenon in which rapid changes of pressure in a liquid lead to the formation of small vapour-filled cavities, in places where the pressure is relatively low. Cause of cavitation is mechanical. Using the Bernoulli equation the pressure is lower where fluid velocity is higher. If the pressure is lower than the vapour saturation pressure than the cavitation bubbles occurs, [6].
Saturation pressure p_{va} depends on type of liquid and temperature. Water at 100°C saturate at pressure of p_{va} = 101.325 kPa, but at room temperature of 20°C saturate at pressure of p_{va} = 2.337 kPa.
When the cavitation bubble or cavity filled with the vapour phase reaches the area of static pressures higher than the evaporation pressure p_{va} and pressure in the liquid rises, vapour bubble implode (negative explosion), Figure. 2, [3].

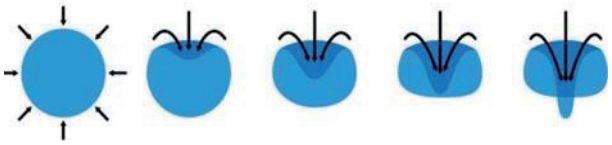

Figure 2. Cavitation process [3]

Collapsing voids that implode near to a metal surface cause cyclic stress through repeated implosion. These results in surface fatigue of the metal causing a type of wear also called "*cavitation*".
Implosion effect is damaged surface and that is called cavitation erosion. Small pores, cracks and holes form on the surface of the wall, which increase over time, not only because of the further mechanical destruction of the material by the implosions of the cavitation bladders, but also by chemical processes that cause accelerated corrosion in the damaged places.
Likewise, these implosions near the wall, in addition to causing erosion of the material, also cause vibrations and noise. Therefore, the influence of cavitation, as a frequent occurrence on the blades of pumps and water turbines, on the wings of a ship's propeller, in hydraulic systems, etc., tends to be reduced. For example, cavitation erosion of ship's propellers is reduced by the use of more resistant materials, by selecting more favourable wing profiles, by installing systems that supply air to the bolt of the bolt, which reduces the rate of implosion, and more, [6].
Cavitation can also be caused by the formation of bubbles that are not filled with liquid vapour, but with gases dissolved in the liquid. Namely, if the pressure in the liquid is higher than the evaporation pressure of p_{va} but lower than the saturation pressure of the gases, gases are generated from the liquid by forming bubbles. When pressure increase again, bubbles disappear without erosion potential because compressibility of gasses dims implosion and hydraulic stroke.
While the vapour cavitation is very rapid, it occurs in micro seconds, gaseous cavitation is slower, and accruement time depends on volume flow.

2. CAVITATION EFFECTS

Cavitation effects, from aspect of the undesirable hydrodynamic process, can divide into mechanical and physical-chemical. This effects can be spotted because of changes of cavitation bubble dimension from first appear than to implosion, Table 1, [6,7].
Table 1. Effects of cavitation [6,7]

Physical - chemical	Mechanical
Pressure and temperature changes)	Cavitation noise
Sonochemical processes	Attenuation of flow caused by forming of vapour bubbles
Sonoluminescence	Strong vibrations
Cavitation corrosion	Material erosion

Cavitation usually has negative effect such as: decrease of efficiency, increase of noise and vibrations, and can cause damage during bubble implosion in front of surfaces. Bubble implosion leads to cavitation erosion. That erosion has unwanted consequences, it is pitting.
It is known that pitting is result of continuous metal surface erosion. The technical standard IEC 60193 prescribes the permissible values of pitting, for example on Francis turbine runners is approx. 40 mm. Average losses on observed blades are 5 kg/m^2 for 10 000 work hours, and repairs have been done every 40 000 working hours, [8].
Relevant international standards does not describe permissible amounts of eroded material depending to runner dimensions, for example; blade thickness. Figure 3. Show examples of damage at Francis turbine runner: a) at hub b) surface cavitation at blades, c) cavitation of inlet edge, [9].

Marija Šiško Kuliš, Nikola Mijalić, Senad Hodžić, Cavitation Detection on Hydraulic Machines, Journal of Energy, vol. 70 Number 3 (2021), p. 25-32
https://doi.org/10.37798/202170328

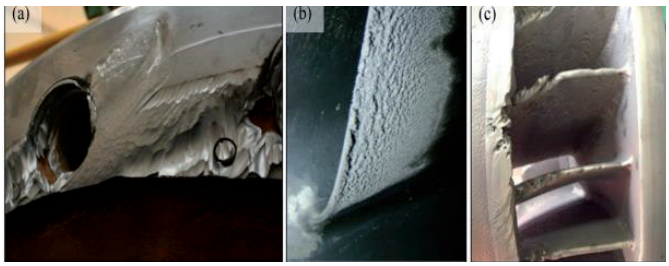

Figure 3. Cavitation erosion damage at Francis turbine[9]

Fig. 4: a) and b) is given example of pump cavitation erosion, and at c) is given example of screw propeller ruined by cavitation erosion, [10] and [11].

Figure 4. Cavitation erosion damage at pump and ships propeller [10, 11]

Erosion damages propagate during the machine operation and can lead to crack occurrence. Timely rehabilitation is necessary. However, if the reconstruction causes a change in the geometry of the blade, such a location can become a source of new separation of fluid flow, i.e. cavitation flow and new erosion. Increased vibration, noise and reduced usability of such a machine must not be neglected. The rate of destruction of solid wall material under the influence of the cavitation process is not always the same and depends on several factors from which they can be separated into:
frequency – higher frequency means faster destruction of materials;
material characteristic;
cavitation bubble dimension – the damage also depends on the size of the bubbles, smaller bubbles have a higher frequency of implosion and often cause more damage than larger bubbles but have a smaller effect on the rest of the system;
hydraulic machine operation condition – cavitation increases frequently when operating modes change, or sudden changes in the system occur.

Electric Power Research Institute, EPRI [12] separate most important causes of cavitation erosion such as: geodetic position of machine, hydraulic turbine design, runner blades profile, machine operation mode, water quality, material etc.
Cavitation cannot be avoided but its effects can be minimized. During the exploitation it is important to take care about EPRI important causes, such as machine operation mode.

3. CAVITATION TYPES

There is a whole series of categorizations of the phenomenon of cavitation, the most common criterion being the location of occurrence, Table 2. The whole series of studies in the focus of research activity has just mentioned criterion.

For example, Franc & Michel specify eight types of cavitation, Franc[13] two types while Ozonek [14] mention four types of cavitation, and Avelan [15],[16] mention eight types of cavitation.
Authors take place of origin as division such as: inlet edge cavitation, surface cavitation, detached vortex cavitation, hub cavitation, inter-blade vortex cavitation, draft tube swirl, Von Karman vortex cavitation etc.
Basic criterion for categorization of cavitation is the type of hydraulic machine on which it occurs: pumps, turbines, marine propellers. Physically, two basic types of cavitation can be determined: vortex cavitation, and bubble cavitation, and their combination, and if the criterion is location in the broad sense, then profile cavitation, gap cavitation and central cavitation are distinguished Profile cavitation will occur when a fluid obstructs a surface at a certain angle, provided that the pressure on one side of the profile is higher and on the other is less than the ambient pressure. Vapour bubbles appear on the profile surface when the pressure drops below the evaporation pressure of the water on the pressure side. The bubbles persist until the pressure is higher than the evaporation pressure, followed by condensation and cavitation erosion. According to the intensity of cavitation, profile cavitation can be defined as: initial stage, advanced stage, super cavitation, Šarc at al.[17].
The cavitation in the clearance is due to the excessive clearance between the rotor and the turbine housing. Previously, the phenomenon of pressure and suction side has been clarified, and if the gap between the impeller blade and the turbine housing is too large, the fluid overflows from the pressure side to the suction side, [5].
Central cavitation generally occurs when the turbine is operating in optimum area.

Table 2. Types of Cavitation - Research Results

Researchers	**Types of cavitation-Research Results**
Franc &Michel [13]	Travelling bubble cavitation, bubble cavitation in the shear layer, localized bubble cavitation, localized attached cavitation hub vortex cavitation, tip vortex cavitation, detached vortex cavitation, surface cavitation.
Bagienski [18]	Surface cavitation, detached vortex cavitation.
Ozonek [14]	Vaporous cavitation, gaseous cavitation, flow cavitation, vibratory cavitation, acoustic cavitation.
Thakkar at al. [19], Escaler at al. [3]	Flow cavitation, traveling bubbles, attach cavities, vortex cavitation.
Li [20]	Leading edge cavitation, flow cavitation, traveling bubbles, ˙draft tube swirl; inter –blade vortex cavitation; Von Karman vortex cavitation.
Avelan [15],[16]	Flow cavitation, traveling bubbles, leading edge cavitation, inlet edge cavitation, inter –blade vortex cavitation, Von Karman vortex cavitation, cavitation whir, hub cavitation.

4. CAVITATION DETECTION TECHIQUES

4.1 General approach

Cavitation detection techniques or methods are numerous and can be categorized according to different criteria, as well as types of cavitation. Thus different authors have different approaches depending on the interest and experience of the researcher. However, it should be noted that cavitation is a phenomenon or characteristic of hydraulic machines that, unfortunately, cannot be transferred with certainty from a model to a prototype of a real plant. It has just been mentioned very important in the development of cavitation detection diagnostics.
If technical and technological conditions are taken as a categorization criterion, then two basic categories can be distinguished: cavitation detection: first, cavitation detection on the model i.e. in laboratory conditions, second, cavitation detection on the prototype i.e. in real plant conditions. Furthermore, if the physical characteristic of the measurement is taken as a categorization criterion, then five basic types of cavitation detection and five methodological groupings are naturally determined: visual methods, acoustic methods, pressure measurements, vibrational methods and ultrasonic method. There is also the division of cavitation detection methods into: direct and indirect methods. The direct method is just visualization while all other methods are indirect.
Methods for detecting cavitation in real plants are based on measurements and analysis of received signals, which is not an easy task since, depending on the shape of the turbine and operating conditions, cavitation always occurs in other places and in other forms. Furthermore, the measured signals on the sensors can be interfered with by noise coming from a part of the plant other than the one we primarily measure. Therefore, it is necessary to carefully locate a good placement of the measuring sensor. For vibration measurement, it is best to

Marija Šiško Kuliš, Nikola Mijalić, Senad Hodžić, Cavitation Detection on Hydraulic Machines, Journal of Energy, vol. 70 Number 3 (2021), p. 25-32
https://doi.org/10.37798/202170328

choose accommodation on the turbine bearing, while pressure is best measured on whole or spiral housings. It is quite important that the measurements and signals obtained are well studied and processed on the basis of a large enough sample to be as accurate as possible. It has already been emphasized in previous sections that cavitation is an unstable phenomenon that raises low-frequency oscillations of pressure as well as pulses of high-frequency pressure. This pressure oscillation depends on the dynamics of the cavities, e.g. shape, type, location, and the pressure pulse occurs due to the implosion of these cavities. Both phenomena emit vibrations and acoustic noise and are propagated by hydrodynamic and mechanical systems. Thus, using suitable sensors that measure vibration and cavitation noise, the phenomena of cavitation in a hydraulic machine can be detected or analysed. Sensors such as accelerometers, acoustic emission sensors are attached to the outer walls of fixed components, and dynamic pressure transducers are mounted on the wet wall, Khakurel [5].

4.2 Literature Review

Several cavitation detection methods have been investigated. Table 3 gives a brief overview of the results of relevant studies of the cavitation phenomenon on hydraulic machines, with particular emphasis on cavitation detection techniques.

Table 3. Research results –cavitation detection

Researcher	Techniques for cavitation detection
Thakkar [19]	Pressure measurement, visual methods, vibration measurements
Koivoula et al. [21]	Visual methods, noise measurements, Pressure measurement and vibration measurements, ultrasonic methods
Šiško [6]	Pressure measurement, acoustic method, vibration measurements,
Li [20]	Pressure measurement, visualising, vibration measurements,
Escaler et al. [22]	Pressure measurement, visual methods, vibration measurements
Cecio et al. [23]	acoustic method
Eich [24]	Pressure measurement, acoustic method
Backe et al. [25]	Pressure measurement, vibration measurements

Pressure, vibration and acoustic pressure measurement are relatively effective methods of cavitation detection.
Grätz et al. [26] and Riedel et al. [27] studied steady-state flow properties in cavitation openings. They obtained parameters that can relatively reliably estimate the occurrence of cavitation in openings.
Wiklund et al. [28] and Myllykylä et al. [29] studied the pumping ability of different pumps. They recorded remarkable results - a decrease in pump output when the suction portion of the pump is cavitated.
Bajić [30] and Eich [24] studied the cavitation noise in the cavitation orifice flow and analysed the recorded acoustic pressure with visual inspection. He concluded that the acoustic method detected the onset of cavitation prior to the visual method. Eich found that at the onset of cavitation, the first responses were in acoustic pressure at high frequencies (> 20 kHz).
Backè et al. [25] used accelerometers in their research. They found that the accelerometer signal indicates cavitation before changing the flow properties at steady state.
Visual inspection in the cavitation orifice stream has been used in several studies (e.g., Šiško [6], Eich [24]). Bajić [30]), In these studies, relatively slow cameras were used; High-speed photography has been used in cavitation research in water tunnels (e.g., Knapp et al. [31]). Slow cameras detect the presence of cavitation, but only a quick photo gives detailed details and information about the size and speed of cavitation cavities.
Koivula et al. [21] have explored a number of useful results by exploring cavitation detection techniques, and a brief summary of the above is given below
Direct cavitation detection is only possible if measuring or detection instruments can access the cavitation zone. This is a very difficult task due to the fact that cavitation as a phenomenon is usually very local in nature. Cavitation detection can only be done directly by checking the existence of cavitation bubbles. Visualization of bubbles in flow passages can be successfully done if light can be scattered in the observation zone. This requires at least two windows for visualization.
Observing the behaviour of ultrasonic waves can reveal the existence of cavities. High flow speed causes ultrasonic waves to deflect. Due to the difficulty in direct detection methods, several indirect cavitation detection methods may be considered. In indirect or indirect methods, measurements are focused on the shock waves generated by the cavitation bubble implosions. Impact waves propagate relatively quickly and far and the position of the sensor is not as limited as in direct measurement. In the observed study, cavitation was indirectly detected by pressure sensors, accelerometers and acoustic instruments. The results showed that the initial phase of cavitation was characterized by intense high frequency pulsations. When cavitation develops, the pulse also extends to lower frequencies.

4.3 Pressure measurement

Pressure measurement is a standard technique for the determination of cavitation on hydraulic machines and is most commonly used in combination with vibration measurement to achieve the most accurate results of the cavitation process. When a bubble enters a high-pressure zone, it vibrates and induces vibrations as well as pressure pulses, Ceccio & Brennen [32].
Escaleret et al. [33] implemented cavitation detection experiments on a Francis turbine by measuring pressure with demodulation amplitude. Figure 5 shows the frequency pulse pressure for the cavitation bubble type and the bez (flow) flow without cavitation. As can be seen, whenever pressure waves are generated due to cavitation, high peaks in the frequency band are obtained.

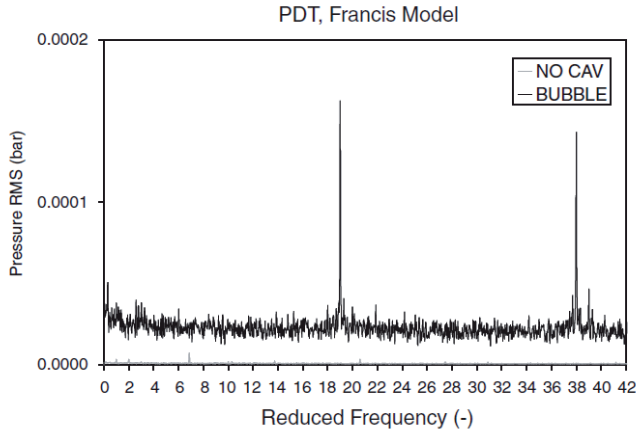

Figure 5. Peak pressure values measured [33]

Pressure changes at draft tube are presented at Figure 6, for different machine operational conditions, and is obvious that the cavitation detects in lower frequency range than in case Peaks are presented when cavitation occur.

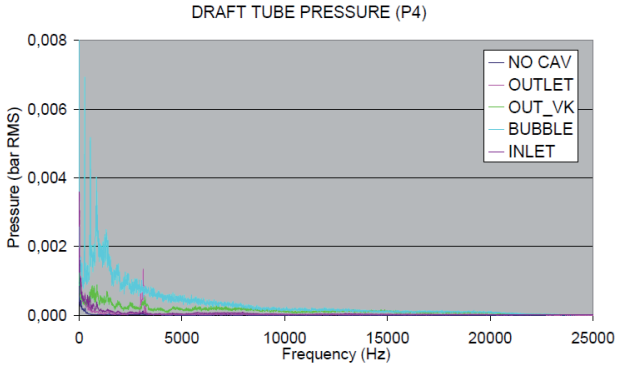

Figure 6. Draft tube pressure at different condition [33]

In their extensive experimental studies, Koivula et al. [21] used, among other things, the pressure measurement method, and they came to a number of conclusions. For example, in indirect cavitation detection methods, the question of the measurement of shock waves caused by cavitation bubble implosions is usually raised. Bubble inhibition is first seen at very high frequencies and therefore very fast pressure transducers are required. The propagation of shock waves continues from the fluid to the environment.

Marija Šiško Kuliš, Nikola Mijalić, Senad Hodžić, Cavitation Detection on Hydraulic Machines, Journal of Energy, vol. 70 Number 3 (2021), p. 25-32
https://doi.org/10.37798/202170328

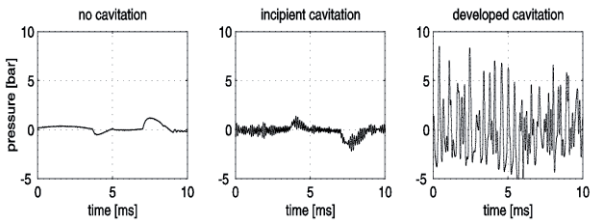

Figure 7. Draft tube pressure for different cavitation periods [10]

The observed study used high - speed transducers to measure peak-to-peak vibration pressure. Figure 7 shows diagrams of time dependence of pressure and the appearance of cavitation rising from left to right.

4.4 Visual method

This method is very popular in last decade especially at hydraulic machines model tests, Šiško [6], Bajić [30]. It is based on the use of stroboscopes and superfast cameras that hang against the Plexiglas window, and sometimes whole sectio
ns of the test station are made of plexiglas, for example, Figure 8.

Figure 8. The test station of the propeller [10]

The test station of the Francis turbine model is shown in Figure 9. In an extensive study of the cavitation phenomenon conducted by Illiescu et al. [1] used LDV (Laser Doppler Velocimetry) systems, optical mirror systems, superfast cameras, diffuser pressure sensors.

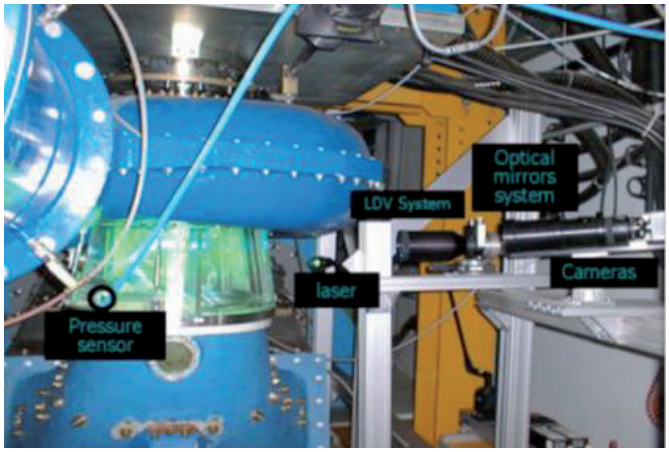

Figure 9. The test station of the Francis turbine model [1]

Avelan [15, 16] investigated cavitation using centrifugal pumps and Francis turbines by visual method.
The results of his research show that the occurrence of cavitation on centrifugal pumps is primar-.ily a function of the flow coefficient ϕ, which depends on the value of the relative velocity and the angle of incidence of the liquid at the inlet edge of the blade. In principle, traveling bubble cavitation occurs on the suction side of the blade while the pressure value is lowest in the rotor throat. At low pump flow rates, the cavitation of the blade inlet edge appears, Figure 10. [15]. Also, at low values of the cavitation number $\dot{\sigma}$, a cavitation swirl appears at the inlet of the pump rotor [16].

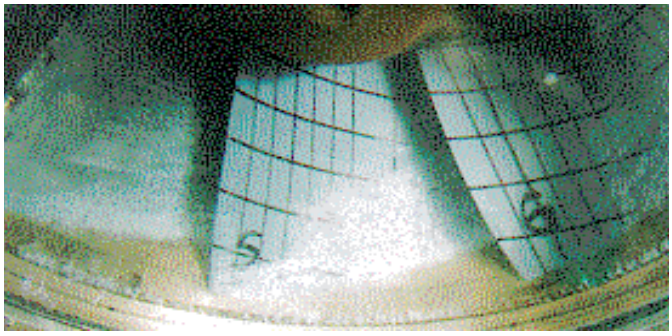

Figure 10. Leading edge cavitation at inlet of pump [15]

Cavitation vortex at Francis turbine draft tube is visualized through the Plexiglas, Figure 10.
A more modern approach to the visualization method is taken by well-known Slovenian researchers Širok et al. [34] who quantified the occurrence of cavitation on Kaplan turbines by the method of computer aided visualization, Figure [11]. Using CCD (Charge-Coupled Device) cameras, stroboscopes and computers (video graphics card) in different turbine operating modes, the occurrence, shape and intensity of the cavitation vortex in the throat of a Kaplan turbine diffuser were analysed.

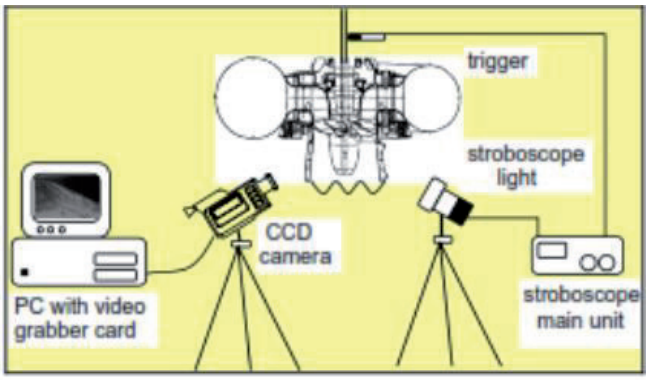

Figure 11. Computer aided visualization [35]

Patel [36] carried out a very interesting study of the occurrence of cavitation at a pump operating in turbine mode. A glass tube was installed at the inlet of the diffuser to visualize the cavitation process, Figure 12.

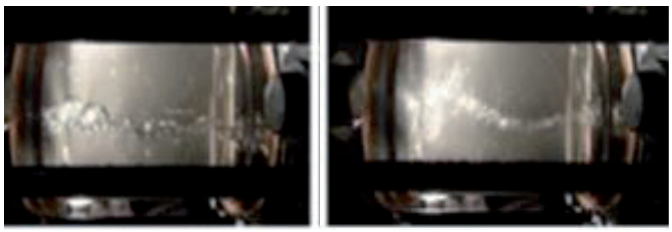

Figure 12. Travelling bubble type cavitation (left) Vortex rope cavitation (right) `[36]

Two types of cavitation are mainly observed: bubble traveling cavitation and cavitation vortex.

4.5 Vibration measurement

Methods for detecting cavitation on real machines are, in principle, based on measurements and analysis of induced signals. Detection of cavitation is not an easy job at all, because it is in the function of several variables, such as the design and operating state of the machine, the type of cavitation, its location and behaviour.
Cavitation vortices and unstable cavities with large oscillating volume cause interference with the main stream and lead to strong pressure pulses within the hydraulic system. This low frequency fluctuation can be detected by means of pressure transducers mounted on the diffuser wall. If the fluctuation intensity is strong, detection can also be performed with structural vibrations. Thus, in this case, the procedure only requires an analysis of the frequency content of the pressure and

Marija Šiško Kuliš, Nikola Mijalić, Senad Hodžić, Cavitation Detection on Hydraulic Machines, Journal of Energy, vol. 70 Number 3 (2021), p. 25-32
https://doi.org/10.37798/202170328

vibration signals in the low frequency range, Bajić [30].
Furthermore, the measured signals can be contaminated by noise from another source whose sources can be quite diverse, i.e. of hydrodynamic, mechanical or electromagnetic origin. Therefore, selecting the most appropriate sensors and measuring position on the machine are fundamental to improving the quality of cavitation detection.
Most of the researchers who deal with these issues agree with this. A number of successful studies have been implemented, for example Escaleret et al. [22, 33] conducted experiments and vibration analysis and proposed to measure the structure of cavitation noise transmitted by liquid. The amplitude of a particular frequency range can be compared for different operating conditions by calculating the intensity of the time signal spectrum. The vibration peaks with amplitude demodulation are shown in Figure 13. High frequency analysis cannot give definitive results as other phenomena can also cause machine vibration and thus perform high frequency amplitude demodulation.

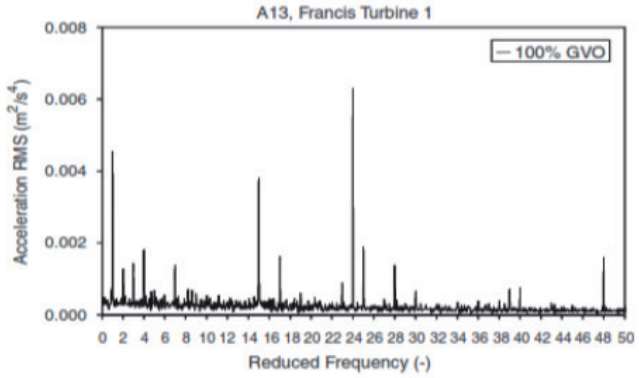

Figure 13. Vibrations peak with amplitude demodulation, [22]

In the observed research, experiments were performed on the Francis turbine model; vibrations were measured using three accelerometers in different positions. One on the shaft and two on the 90 degree bearings. Different acceleration values within the given frequency range were measured for different openings of the control blades and it was concluded that the turbine was separated from its BEP (Beam Experimental Platform), higher peaks were obtained at the frequency of 6 kHz as shown in Fig. 14 and Fig.15. where the Guide Vane Opening [%] is the opening of guide vane mechanism.

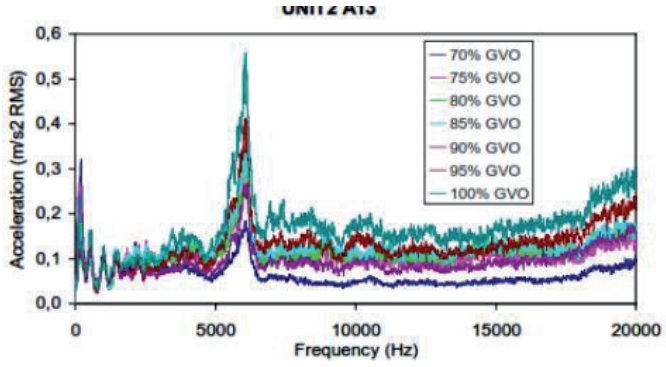

Figure 14. Vibration at bearing for different GVO,[22]

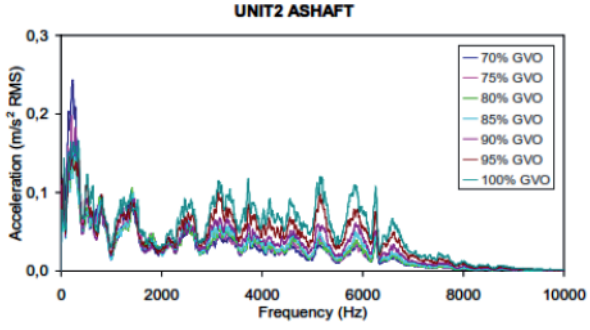

Figure 15. Vibration at shaft for different GVO,[22]

Koivula et al. [21] also explored the method of detecting cavitation by measuring vibrations.

4.5 Cavitation noise measurement

Studying vibrations, acoustic emissions, and dynamic pressure levels in a high frequency range is a well-known technique for detecting cavitation. The amplitudes of the set frequencies can be compared for different operating conditions by computing the time signal spectrum. A steady and sharp increase in frequencies when compared to a state where there is no cavitation can indicate the presence of cavitation. The use of acoustic emission sensors allows this analysis to be extended to upper frequencies that accelerometers cannot reach. The information we get is sometimes irrelevant because sometimes we get signals and frequencies from other parts of the system or environment. Therefore, it is necessary to use an amplitude demodulation technique to improve diagnostics.
Eskaler et al. [22, 3] performed experiments on a Francis turbine model by measuring acoustic emission. The figure shows the measured acoustic emissions for the different openings of the control blades (A0) for the frequency range from 0 kHz to 20 kHz. The values increased with increasing GVO GVO with the exception of the abrupt fall of 90% measured by the accelerometers. Bajić [30] performed measurement on Kaplan turbine, Dubrava HPP – Croatia.
Patel et al [37] performed acoustic emission analysis on a pump as a PAT (Process Analytical Technology) turbine operating at different speeds to detect cavitation.
Koinvoul et al. [21] also used an acoustic method in their extensive cavitation studies. A number of conclusions have been reached, for example: more extensive information on cavitation occurrence is obtained when measuring cavitation noise with a large range of high frequencies. Moreover, if the results are plotted as a frequency spectrum, the onset and development of cavities is clearly seen. The measured frequency spectrum of the acoustic pressure is shown as a 3D graph in Figure 16. Over a period of 3s, one can clearly see the moment of cavitation occurrence in a sharp increase in acoustic pressure at high frequencies (> 8 kHz). When cavitation develops, the acoustic pressure also extends to lower frequencies. The same trend is observed in spectral analysis when measuring the pressure and vibration of the origin and development of the cavitation process.

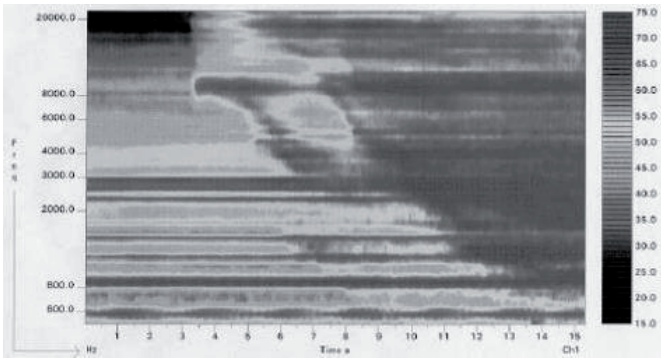

Figure 16. Frequency spectrum of acoustic pressure [21]

Ceccio et al. [23] and [32] showed that cavitation noise analysis is a useful tool for investigating the properties of cavitation phenomena. It is easy to measure the noise structure in a turbine, while it is very difficult to measure noise transmitted to the fluid because it is impossible to fit a pressure sensor in the turbine rotor. It must also be borne in mind that cavitation noise cannot be directly measured, since the signal strength as they propagate is attenuated. Nevertheless, the spectral content of high frequencies and modulating frequencies can be used to detect cavitation.

4.6 CFD Analyses

CFD (*Computational Fluid Dynamics*) is branch of fluid mechanics which uses numerical analyses and solving *Navier-Stokes* equations for predicting and solving problems in fluid mechanics. Computers are used to calculate fluid flow and interaction between liquid and vapour phase with boundary conditions.
In last time CFD is used often for solving most complex problems in turbomachinery worldwide. Supercomputer with powerful processor and better overall performances are needed for better results. And that

Marija Šiško Kuliš, Nikola Mijalić, Senad Hodžić, Cavitation Detection on Hydraulic Machines, Journal of Energy, vol. 70 Number 3 (2021), p. 25-32
https://doi.org/10.37798/202170328

is the problem because the supercomputer cost too much. For cavitation problems CFD can predict fields where cavitation will appear but cannot predict the effectiveness of cavitation erosion.
Two are mean principles in numerical solving of cavitation problems in CFD: first is *mixture model* and the second one is *eulaerian model*. There are lot numerical models implemented in these two mean principles such as: 1) *Singhal* i sur. – better known like *Full Cavitation Model*, 2) *Zwart-Gerber-Belamri*, 3) *Schnerr* & *Sauer*, and like *Kunz*-a... The most common models for cavitation modelling are IFM (*Intensity Function Method*), GLM (*Gray Level Method*), DBM (*Discrete Bubble Method*). There is a combination of GLM i DBM method and that is EPM (*Erosive Power Method*).
Numerous investigators for the first phase investigations use this method. Sedlar et al. [38] described new model for cavitation erosion prediction using numerical modelling of turbulent cavitation. They analysed dynamic behaviour of cavitation bubbles which occur with gradient of pressure change in hydraulic machine. Potential cavitation erosion model is based on energy dissipated by bubble. Energy which has dissipated through bubbles collapse is used for shock wave modelling which spreads from bubble. Part of shock wave energy transmitting to surface represent erosion potential.
Nohmi et al. [39] are using CFD analysed cavitation processes for centrifugal pumps. They used two models: two-stage model for compressible fluids, better known as TE model, and other CEV (*Constant Enthalpy Vaporization*) model. Both models have same results of prediction, Figure 17.

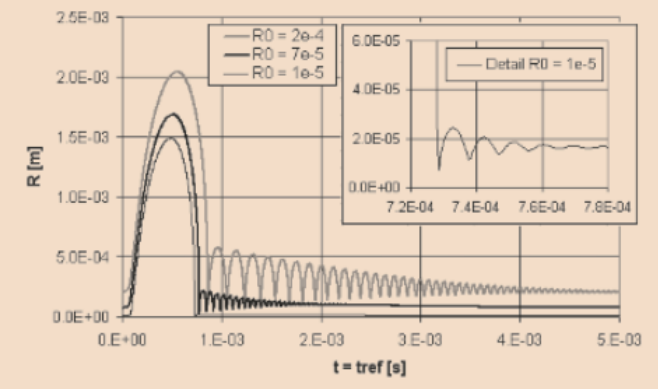

Figure 17. Bubble collapsing [39]

Both models show suction head drop when cavitation occurs. Analyses have shown that for higher fluid velocities model need to be modified. Iosif et al. [40] presented an explicit numerical one model based on finite element method and dual reciprocal method. They suggested using a model to transform 3D flow into 2D problems for an ideal noncompressible fluid. They solved the axisymmetric potential flow using FEM (*Finite Element Modelling*) by determining the distribution of pressure and velocity along the stream. The results were analysed for a reversible hydraulic machine and showed different flow values previously used to determine the cavitation characteristic and the sensitivity curve.

5. CONCLUSION

Cavitation is the undesirable phenomenon at hydraulic machines that can be predicted and with various techniques reduced but never entirely avoided.
Many researchers used various techniques such as visual method, pressure and cavitation noise measurements, CFD methods for predicting and analyses of cavitation. Also techniques are used for prediction cavitation erosion potential.
It is rare to use only one technique. Usually two, three or four techniques are used for reliably prediction.
For model test visual method is most dominant method, but for hydraulic machines in operation pressure and vibration measurement are most used techniques.
Several researchers noticed that the cavitation can be registered firstly with pressure measurement method than with visual method.
It is widely known that the cavitation characteristic can't be translated from model test to real machines. That means it is necessary to invest more time to determine the cavitation characteristic.
Numerical CFD simulations can reliably determine cavitation but cannot predict cavitation erosion with great accuracy. In future the CFD simulations in turbomachinery will be in progress and potentially dominant in determination of cavitation characteristic.
Each of the methods for cavitation detection on hydraulic machines has advantages and disadvantages and there are gaps for improvement. However, the main problem is fact that there are no exactly formula for linking relation from laboratory cavitation test to prototype cavitation, until now. Moreover, real cavitation characteristics can only be obtained on hydraulic machines in operation in the real facilities. Following this, the acoustic method is easy to apply and has significant potential in linking laboratory tests and tests on prototypes. So, future research should put focus on acoustic method and closer cooperation between scientists and engineers involved in the maintenance of hydraulic machines.

Marija Šiško Kuliš, Nikola Mijalić, Senad Hodžić, Cavitation Detection on Hydraulic Machines, Journal of Energy, vol. 70 Number 3 (2021), p. 25-32
https://doi.org/10.37798/202170328

REFERENCE

[1] Iliescu M. S., Ciocan G. D., Avellan F., "Analysis of the Cavitating Draft Tube Vortex in a Francis Turbine", Journal of Fluids Engineering, FEBRUARY 2008, Vol. 130. 2008

[2] https://www.uni-due.de/ISMT/ismt_cavitation_en.shtml (25.04.2019.)

[3] Escaler X., Farhat M., Ausoni P., Egusquiza E., Avellan, F., "Cavitation monitoring of hydroturbines: Tests in a Francis turbine model," Sixth International Symposium on Cavitation CAV2006, Wageningen, The Netherlands, 2006

[4] Aktas B., "Systematic Experimental Approach to Cavitation Noise Prediction of Marine Propellers", This dissertation is submitted for the degree of Doctor of Philosophy, School of Marine Science and Technology Newcastle University.2016

[5] Khakurel N., "Analysis on effects and limitations of cavitation in design and operation of Francis turbine", Master of Science in Energy Systems, Aachen University of Applied Sciences, Campus Jülich. 2016

[6] Šiško M., "Kavitacija na rotorima Francisovih turbine", magistarski rad, Fakultet strojarstva i brodogradnje, Zagreb. 1997

[7] Khurana S., Navtej and Hardeep Singh, N and S., "Effect of Cavitation on Hydraulic Turbines- A Review", International Journal of Current Engineering and Technology ISSN 2277 – 4106. 2012

[8] IEC 60609 -1. Hydraulic turbines, storage pumps and pump-turbines Cavitation pitting evaluation Part 1: Evaluation in reaction turbines, storage pumps and pump-turbines, 2004

[9] Teran L. A., Rodriguez S. A., Laand, S., Jung, S., "Interaction of particles with a cavitation bubble near a solid wall", arXiv:1810.12148v1 [physics.flu-dyn] 29 Oct 2018

[10] https://www.pumpsandsystems.com/staff-blog/3-must-read-articles-about-cavitation (23.04.2019.)

[11] https://www.vicprop.com/store2/blog/cavitation-erosion (20.04.2019.)

[12] EPRI, Electric Power Research Institute, "Cavitation Pitting Mitigation in Hydraulic Turbines". Volume 1: Guidelines and Recommendations, Palo Alto, CA, USA.1986

[13] Franc J.P., Michel J.M., "Fundamentals of cavitation", Kluwer Academic Publishers, Dordrecht. 2004

[14] Ozonek J., "Application of Hydrodynamic Cavitation in Environmental Engineering". Taylor & Francis Group, London. 2012

[15] Avellan F., "Introduction to cavitation in Hydraulic Machinery", H.M.H 2004, 6th International conference on Hydraulic Machinery and Hydrodynamics, Timisoara, Romania. 2004

[16] Avellan F., "Introduction to cavitation in Hydraulic Machinery", H.M.H 2004, 6th International conference on Hydraulic Machinery and Hydrodynamics, Timisoara, Romania. 2004

[17] Šarc, A., Petkovšek, M., Stepisnik-Perdih, T, Dular, M., "The issue of cavitation number value in studies of water treatment by hydrodynamic cavitation", Ultrasonics Sonochemistry. 2016

[18] Bagienski J., "Cavitation in a device with water and heat", Wydawnictwo Politechniki Poznanskiej, Poland. 1998

[19] Thakkar N., Chaudhari S., "Cavitation Detection in Hydraulic Machines": A Review, International Journal on Theoretical and Applied Research in Mechanical Engineering (IJTARME). 2015

[20] Li S.C., "Cavitation of Hydraulic Machinery", University of Warwick, UK.2000

[21] Koivula T, Ellman A. & Vilenius M., "Experiences on cavitation detection methods". in Proceedings, XVI IMEKO World congress, IMEKO 2000, September 25-28, 2000, Vienna, Austria. pp. 49-54. 2000.

[22] Escaler X., Egusquiza E., Farhat M., Avellan F., "Vibration Cavitation detection using Onboard Measurements" Cav03-OS-6007, Fifth International Symposium on Cavitation, Osaka, Japan.2003

[23] Ceccio S. L., Brennen, C. E., "Observations of the dynamics and acoustics of travelling bubble cavitation", Journal of Fluid Mechanics 233 (1991) 633– 660.1991

[24] Eich O., "Entwicklung geräuscharmer Ventile der Ölhydraulik. Dissertation TH Aachen" .157p.1979

[25] Backè W., Berger, J., "Kavitationserosion bei HFA-Flüssigkeiten". O+P "Ölhydraulik und Pneumatik" 28 Nr. 5. 5 p.1984

[26] Grätz U., "Berechnung des Volumenstromens unter Berücksichtigung des Kavitationseinflusses". O+P "Ölhydraulik und Pneumatik" 39 Nr.4. 5 p. 1995

[[27] Riedel H.-P., "Untersuchungen von Kavitationserscheinungen an hydraulischen Widerständen". Dissertation RWTH Aachen.1973

[28] Wiklund P.-E., Svedberg, G., "Cavitation Properties of an Axial Piston Pump Using a Vegetable and a Mineral Oil". 9th Bath International Fluid Power Workshop. Bath. 13 p. 1996

[29] Myllykylä J, "Semi-Empirical Model for the Suction Capability of an External Gear Pump". Tampere University of Technology, 1999. Dissertation TUT. 71p.1999

[30] Bajić, B. "Multidmenzionalna dijagnostika i monitoring kavitacije – Metode za mali broj lopata radnog kola-Primjena na HE Dubrava". Journal of Energy - Energija, Vol. 51, no. 5, pp.394-397.2002

[31] Knapp R., Daily W., Hammitt F., "Cavitation". McGraw - Hill. 578 p. USA.1970

[32] Ceccio S. L., Brennen, C. E., "Partial cavity flows. Part 1. Cavities forming on models without spanwise variation" , Journal of Fluid Mechanics) 61-41.1991

[33] Escaler X., Egusquiza E., Farhat M, Avellan F., Coussirat M., "Detection of cavitation in hydraulic turbines", Mechanical systems and signal processing 20(2006) 983-1007.USA.2004

[34] Širok B., Dular M., Novak M., Hočevar M., Stoffel B., Ludwig G., "Influence of Cavitation Structures on Erosion of Symmetrical Hydrofoil in a Cavitation Tunnel", Journal of Mechanical Engineering, Ljubljana 2002.

[35] Sirok B., Novak M. Hocevar M., Prost, J. "Visualization Monitoring of Cavitation in Water Turbine" . Conference proceedings 12th Internationale Seminar on Hydropower Plants, Vienna, Vienna University of Technology - Institute for Waterpower and Pumps, 2002, p.305-314. 2002

[36] Patel N.K., "Cavitation and Draft Tube Analysis of PAT", M Tech report, Institute of Technology, Nirma University. 2014

[37] Patel N.K,"Experimental Investigations of Cavitation Characteristics of Pump Running in Turbine Mode", Journal of Energy Engineering February 2017 Volume 143, Issue 1. 2017

[38] Sedlar M., Zima P. Muller M., "CFD Analysis of Cavitation Erosion Potential in Hydraulic Machines", 3rd IHAR International meeting of the workgroup on Cavitation and Dynamic problems in Hydraulic Machinery and Systems, Brno, Czech Republic. 2014

[39] Nohmi M., Goto A., Iga Y., Ikohagi T., "Cavitation CFD in a Centrifugal Pump", Fifth International Symposium on Cavitation (Cav2003) Osaka, Japan.2003

[40] Iosif and Sarbu, "Numerical modeling of cavitation characteristics and sensitivity curves for reversible hydraulic machinery", Elsevier, Engineering Analysis with Boundary elements. Vol. 41, pp. 18-27. 2014

ENERGIJA